Projections • 16. Measuring the City: The Power of Urban Metrics

Urban MorphoMetrics + Earth Observation: An integrated approach to rich/extra-large-scale taxonomies of urban form

Sergio Porta[1] Alessandro Venerandi[1] Alessandra Feliciotti[1]
Shibu Raman[2] Ombretta Romice[1] Jiong Wang[3] Monika Kuffer[3]

[1]Urban Design Studies Unit, Department of Architecture, University of Strathclyde, Glasgow, UK.,
[2]Welsh School of Architecture, Cardiff University, Cardiff, UK.,
[3]Faculty of Geo-Information Science and Earth Observation (ITC), University of Twente, Enschede, The Netherlands.

MIT Press

Published on: Jun 20, 2022

URL: https://projections.pubpub.org/pub/vfwe0fdj

ABSTRACT

Homogeneous fine-grained patterns of urban form represent identifiable areas in cities and allow their classification. Urban morphology uses the concepts of “morphological period,” “urban tissue,” or “character areas” to link fine-grained homogeneity of form to historical origins and the social and economic characters associated with them. However, identifying such fine-grained spatial patterns is a labor-intensive, specialist operation, thus limiting replicability and scalability. Therefore, comprehensive urban form classification has rarely been conducted at a very large scale, hindering our understanding of how form contributes to social, economic, and environmental urban dynamics.

With expanding capacity in geo-computation, urban analytics, and Earth Observation (EO) technology, new numerical approaches to the large-scale and detailed description of urban form have recently emerged. However, limitations due to availability, quality, and consistency of data still apply. We present an integrated approach to extra-large-scale urban form analysis that combines a novel Urban MorphoMetrics (UMM) method for the generation of rich and unsupervised urban form taxonomies with advanced EO feature-extraction techniques.

UMM utilizes extremely parsimonious input information to generate a comprehensive set of urban form characters for three morphometric elements (buildings, streets, and plots), over six categories (dimension, shape, spatial distribution, intensity, connectivity, and diversity) and three scales (small, medium, and large). All characters are measured at the building level and clustered into distinct homogeneous urban types, thus creating a comprehensive taxonomy of urban form. UMM is applicable across cases, allowing individual type profiling and cross-case comparison. We illustrate UMM outputs across a range of case studies covering formal and informal urban areas in sharply different geographical and cultural contexts worldwide. The results demonstrate an encouraging ability to map urban form in cities in ways that relate to historical origins, land uses, and other validating geographies.

The method also shows a pathway to address varying degrees of availability, quality, and consistency of input data, which is commonly poor, for example, in informal settlements. Explorations of ways to resolve this issue include integrating UMM with EO. The latter offers a way to generate globally consistent input data from freely

accessible repositories, hence ensuring full control of quality and consistency. Thus, we show that our first efforts to combine UMM and EO data into an integrated UMM+EO process are suitable for use at a global scale.

Introduction

Origins, nature, and context of Urban MorphoMetrics

Urban MorphoMetrics (UMM) is a method of urban morphology analysis aimed at extracting the inner spatial patterns that distinctively characterize urban places in a numerical form. The method is specifically designed to bring together richness of description with extra-large-scale coverage for the generation of a systematic hierarchical taxonomy of urban form. This is achieved via advanced geo-data processing techniques paired with an analytical architecture that is purposefully designed for scalability.

Early ideas at the root of UMM were proposed by one of the authors of this paper in the years 2005–2006 to students of the Polytechnic of Milan. The aim was to teach urban designers how to identify fundamental spatial patterns that have proved adaptable over time from existing urban structures. It also aims to allow them to use the same information in their design proposals for new areas of urban expansion or regeneration projects. Those early attempts were based on students' labor-intensive surveys at the scale of the urban block, rooted in both the Conzenian and Muratorian traditions of urban morphology (Cataldi, Maffei, and Vaccaro 2002; Whitehand 2007). The term "urban morphometrics" appeared about five years later (Carneiro et al. 2010; Porta 2011) after the re-establishment of the leading research team at the University of Strathclyde in Glasgow. Since the very beginning, pivotal elements have been 1) connecting analysis and design; 2) comprehensive, numerical description; and 3) an evolutionary approach to urban change.

A first attempt at developing a truly systematic and scalable turn to this approach started in 2013 and made an early appearance in 2015–16 (Dibble et al. 2016), with a more mature one three years later (Dibble et al. 2019). In the meantime, further developments had started (Fleischmann 2019; Fleischmann et al. 2020, 2021b; Fleischmann, Romice, and Porta 2021a), leading to a comprehensive prototype. As recently acknowledged in the twenty-eighth International Seminar of Urban Form conference, a wide and diverse area of urban morphometric studies is now rapidly emerging, including the UMM method presented in this paper.

Urban MorphoMetrics (UMM)

The UMM methodology illustrated in this work was developed in Venerandi et al. (2021) and derived from Fleischmann et al. (2021b). In this section, we present its main features and refer the reader to these two works for more detailed explanations. UMM is based on combining 300+ spatial characters of urban form in six main categories: dimension, shape, distribution, intensity, connectivity, and diversity. The rationale behind the selection of characters is *comprehensiveness*: aiming at the largest possible set of characters proposed in literature and technically viable in this specific research framework. This is preferred to selecting a limited number according to predetermined theories or criteria. All characters are generated from only two input data layers: buildings (with heights) and the street network. The computation of the characters is unsupervised and replicable for the purposes of scalability and rigor. The spatial unit of analysis is the *morphological cell*, a geometric derivative of the Voronoi tessellation generated from the building footprint (Fleischmann et al. 2020), a proxy of the plot or cadastral parcel.

UMM generates 74 primary characters and 296 (74x4) contextual characters. The former describe streets, cells, and buildings, as well as their relationships at three different scales: S (the element itself), M (the element and immediate neighboring elements), and L (the element and neighboring elements within *k*-th order of contiguity) (Fleischmann et al. 2021b). Examples of primary characters are the meshedness of the street network, the coverage area ratio, and the building elongation. We refer the reader to Table 1 in the Appendix for the full list. To account for the context around each morphological element, four contextual characters are derived from each primary character: the interquartile mean, the interquartile range, the interdecile Theil index, and Simpson's index. The first is the average computed on the values between the first and third quartile of the distribution. The second is the range in values of the same values. The third is a measure of local inequality. The fourth is an index of the values' heterogeneity (2021b).

The taxonomy is then generated by applying agglomerative hierarchical clustering (AHC) (Rokach, Lior, and Oded 2005) to the contextual characters. AHC is a hierarchical method of cluster analysis, which constructs a tree (dendrogram) of clusters, here named "urban types" (UTs), starting from single morphological cells up to a main branch. A connectivity constraint is used to avoid inhomogeneous classification of individual outliers in areas overwhelmingly characterized by one UT. The optimal number of UTs is identified using a silhouette diagram, a heuristic method

for the interpretation and validation of consistency in cluster analysis (Rousseeuw 1987). Postprocessing workflows of consecutive rounds of clustering and silhouette can be implemented on the values pertaining to specific UTs to better differentiate subpatterns using local knowledge. A final dendrogram, fundamental for assessing levels of similarity between UTs, is built by recomputing the tree starting from the cluster centroids of each UT. The same technique of dendrogram merging can be utilized to compare UTs across multiple cities, hence achieving a systematic and rigorous account of morphological similarities and uniqueness of urban fabrics across a potentially unlimited geographical extent. An example of cross-case dendrogram merging can be found in (2021b).

In the following sections, we first illustrate the individual application of UMM to two European case studies, Amsterdam (NL) and Bologna (IT), with optimal data. Second, we illustrate how it can be applied to Kochi (IN), where there is limited data availability. Third, we show the potential of EO to support UMM in regions with no data availability, by applying an integrated EO+UMM approach to a sample area in Nairobi (KE), which is characterized by an urban divide between formal and informal areas as well as a range of types of informal settlements. Fourth, we provide a discussion on the potential and limitations of UMM and the integrated EO and UMM workflow.

Applications of UMM

In this section, we present the outcomes of the application of UMM onto Amsterdam, Bologna, Kochi, and a sample area in Nairobi. These four case studies belong to very distinct geographical/cultural contexts, they grew by following different design paradigms, and they currently have different levels of data availability. To help orient the reader, Table 1 presents a summary of their main features.

Case study	**General info (country, metro population)**	**Data used**	**Interest**
Amsterdam	The Netherlands, 2,480,394	Buildings with heights, street network (official data sets)	Medieval origin, mixing different planning styles

Bologna	Italy, 1,017,196	Buildings with heights, street network (official data sets)	Pre-Roman origin, mixing wide range of planning styles
Kochi	India, 2,119,724	Buildings (manually extracted)	Generalized informal urban development
Nairobi (sample area)	Kenya, 10,400,676	Buildings (automatically extracted)	Relatively recent foundation, presence of informal settlements

Table 1. Case studies, general information, data availability and particular points of interest for the application of UMM.

Amsterdam (NL)

Amsterdam was originally a fishing village, dating roughly to the twelfth century. In the seventeenth century, it became one of the most influential port cities in the world due to its excellence in finance and trade. In this same period, an extensive reshaping of the city took place through the construction of four concentric half-circles of canals, deemed necessary for defense, water management, and transport purposes. In the nineteenth and twentieth centuries, several new expansion plans were proposed and developed, in particular, the Plan Zuid and West, designed by H. P. Berlage in the nineteenth-century tradition, and modernist expansions located in the western, southeastern, and northern fringes. These latter developments purposely depart from any historical reference, featuring large stand-alone housing complexes surrounded by extensive open areas. Amsterdam's layered morpho-historical complexity makes the city an interesting case study for the application of UMM.

AHC was recursively applied to the full set of 296 contextual characters previously computed in Fleischmann et al. (2021b): out of 30 possible UTs, 14 were optimal, combining the best silhouette score with the highest level of detail. In Figure 1, we present the numerical taxonomy of Amsterdam, where building/cell colors uniquely identify the UTs. Notably, similarity of color hues expresses similarity of detected patterns of urban form, as in the accompanying dendrogram (Figure 2).

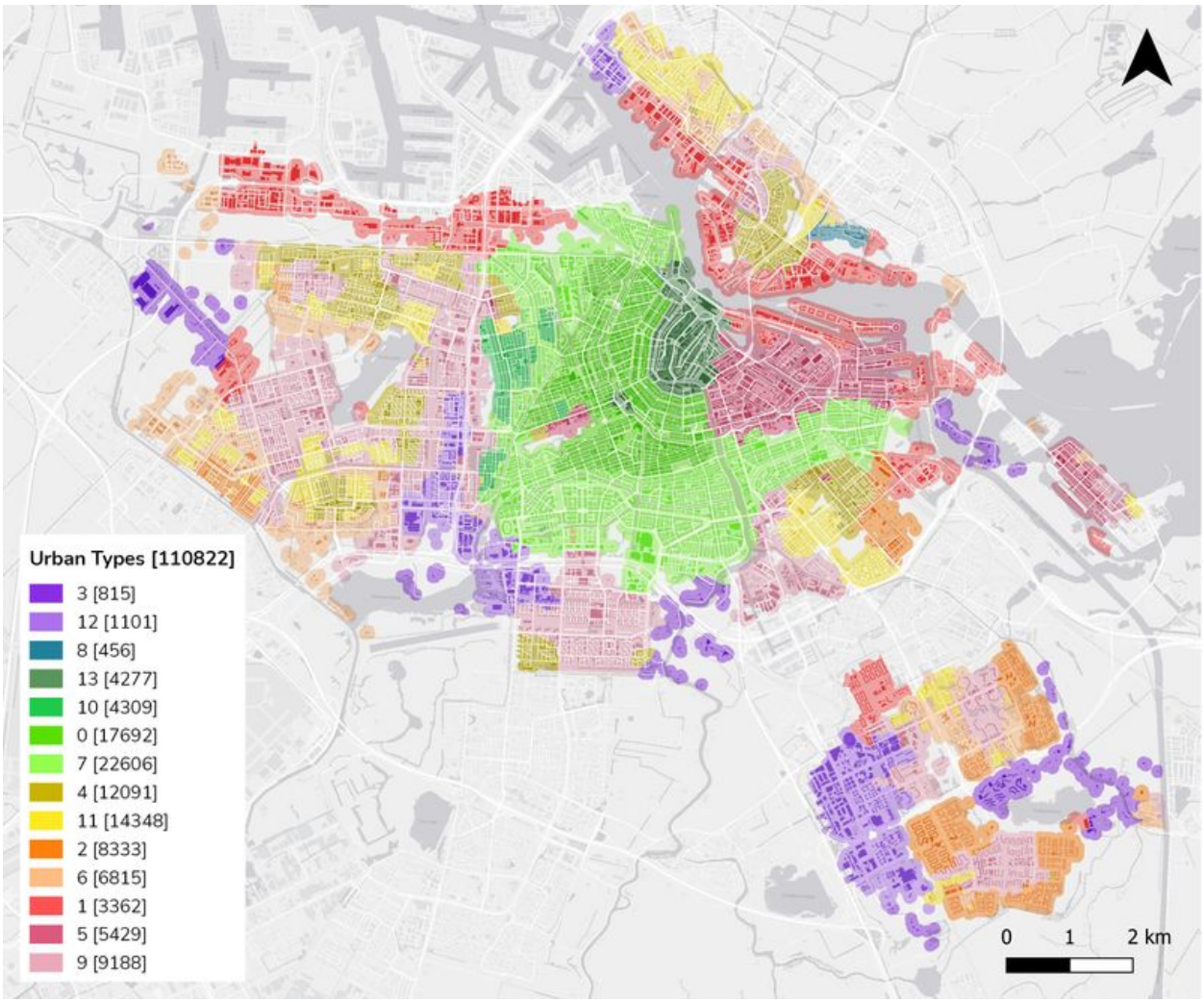

Figure 1

Morphometric taxonomy of Amsterdam (14 UTs): building/cells' colors identify UTs. Similarity of colors reflect similarity of form patterns. Source: Authors' own elaboration based on data from Dukai, Balázs. 2018. "3D Registration of Buildings and Addresses (BAG) / 3D Basisregistratie Adressen en Gebouwen (BAG)." 4TU.ResearchData. Available at: https://data.4tu.nl/collections/_/5065523/1 (accessed 3 November 2021).

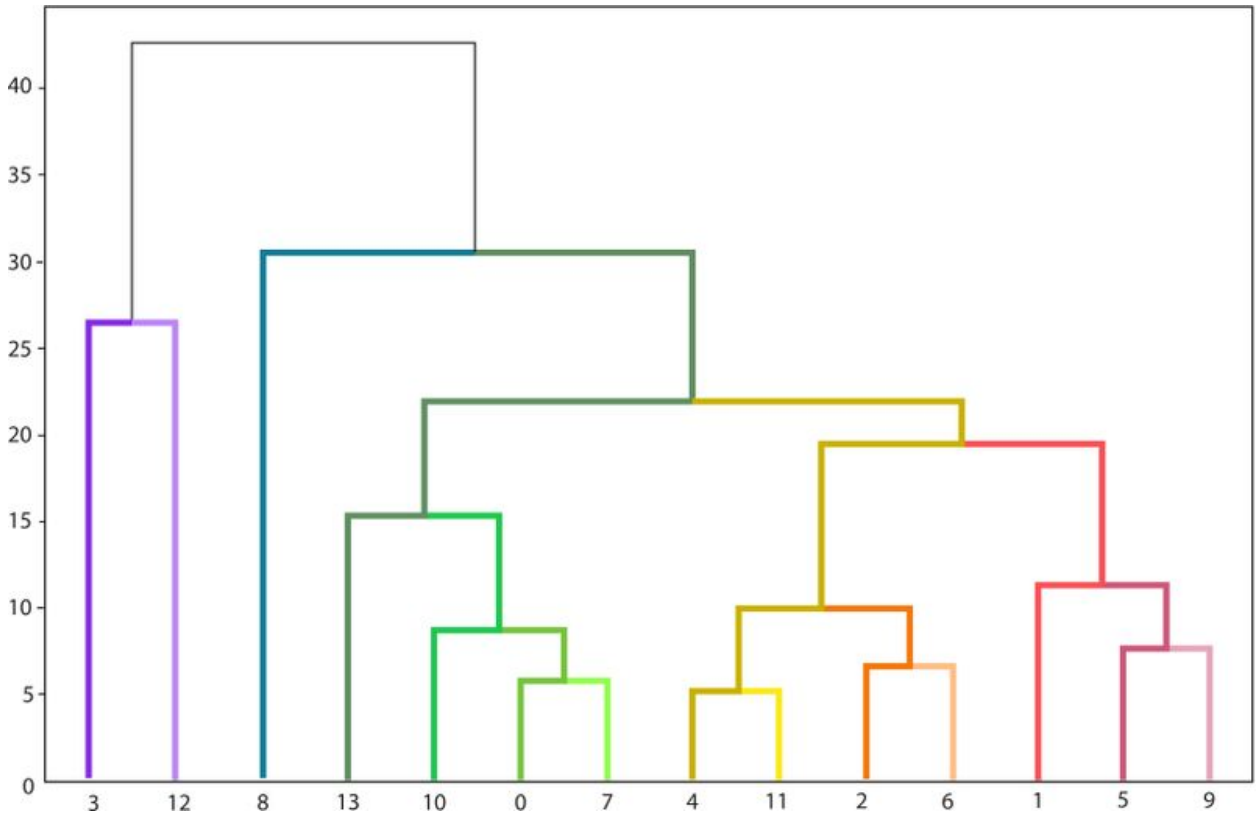

Figure 2

Dendrogram of the 14 UTs of Amsterdam: similarity between UTs is expressed by both the *y*-value of their point of conjunction (the lower the value, the higher the similarity) and the similarity of their color. Source: Authors' elaboration.

The most noticeable aspect of the taxonomy of Amsterdam is the stark split between modernist/industrial urban fabrics, at the extremes of the dendrogram (UT3, UT12, UT1, UT5, UT9 in Figure 2), and the most historical ones, in the middle of it (UT13, UT10, UT0, UT7). By inspecting the values of the cluster centroids of the contextual characters diverging the most from the average across UTs, we observe that the former group is mainly characterized by remarkably coarse and incoherent patterns, large morphological elements up to 6.5 standard deviations more than the average for Amsterdam, isolated, compact, bulky buildings, low local street network connectivity, and diversity of cell areas and building–cell alignments. Bullewijk, located southeast of the main center, classified UT12, is an example of this type of urban fabric. As for the latter group (UT13, UT10, UT0, UT7), the taxonomy distinctively captures different stages of Amsterdam's historical development. UT13, for example, corresponds to the innermost historical core (up to 1850) characterized by an organic, compact, diverse and dense urban fabric, large range of height-to-width ratios, high and large range of built-up densities, high local street network connectivity, high coverage ratios, and low building footprint complexity, with elongated shapes and oblique corners with different

degrees. UT0 partly corresponds to the 1851–1950 city development and, while it shares some of the features of UT13, such as high and large range of built-up densities, high coverage ratios, and more elongated buildings, it also shows differences that are typical of late-nineteenth-century urban planning, such as large proportions of four-way intersections and higher local accessibility. Amsterdam is an example of a data-rich city for which UMM shows a good capacity to capture the inherent correspondence between historicity and morphological similarity embedded in the city's built form.

Bologna (IT)

Bologna has two features that make it particularly interesting for UMM. The first is the presence of two markedly different urban forms: 1) the ancient historical core, which dates to the Etruscan and Roman settlements of the sixth and seventh and centuries B.C., is encircled by a ring road that follows the path of the former medieval city wall erected in the eighth century and demolished in the early twentieth century A.D., and features a mix of midrise medieval and renaissance buildings, small courtyards and squares, and narrow roads flanked by public arcades and 2) a large suburban expansion completely surrounding the historical core, most of which was built in successive waves starting in the early twentieth century. This vast area can be roughly subdivided into two subparts: 1) the inner suburb, built in the first half of the 1900s, characterized by a regular, gridded pattern and street-facing buildings of gradually declining densities, and 2) the outer periphery, featuring specialist districts (i.e., commercial, industrial or large transportation hubs) as well as isolated large-scale social housing estates comprehensively planned and built between the mid-1950s and the 1960s, with high-rise buildings and large traffic roads.

The second feature is its geomorphology. Due to its location between the Po Valley and the Apennines, Bologna's topography changes considerably, from the northern part built on a largely flat piece of land that belongs to the high Po river valley to the southern part on the steep lower slopes of the Apennines, where urbanization was strongly constrained by the local orohydrography.

Data on building footprints and the street network were downloaded for free from the official Geo-Portal of the Emilia Romagna Region.[1] We computed the 296 contextual characters from this data and recursively applied AHC on them to determine the optimal number for solutions of up to 20 UTs. After checking the silhouette score and the level of detail, we identified 11 as the optimal number of UTs. Both the spatial

distribution of the UTs (Figure 3) and the dendrogram (Figure 4) appear to accurately capture the main phases of the morphological history of this ancient city.

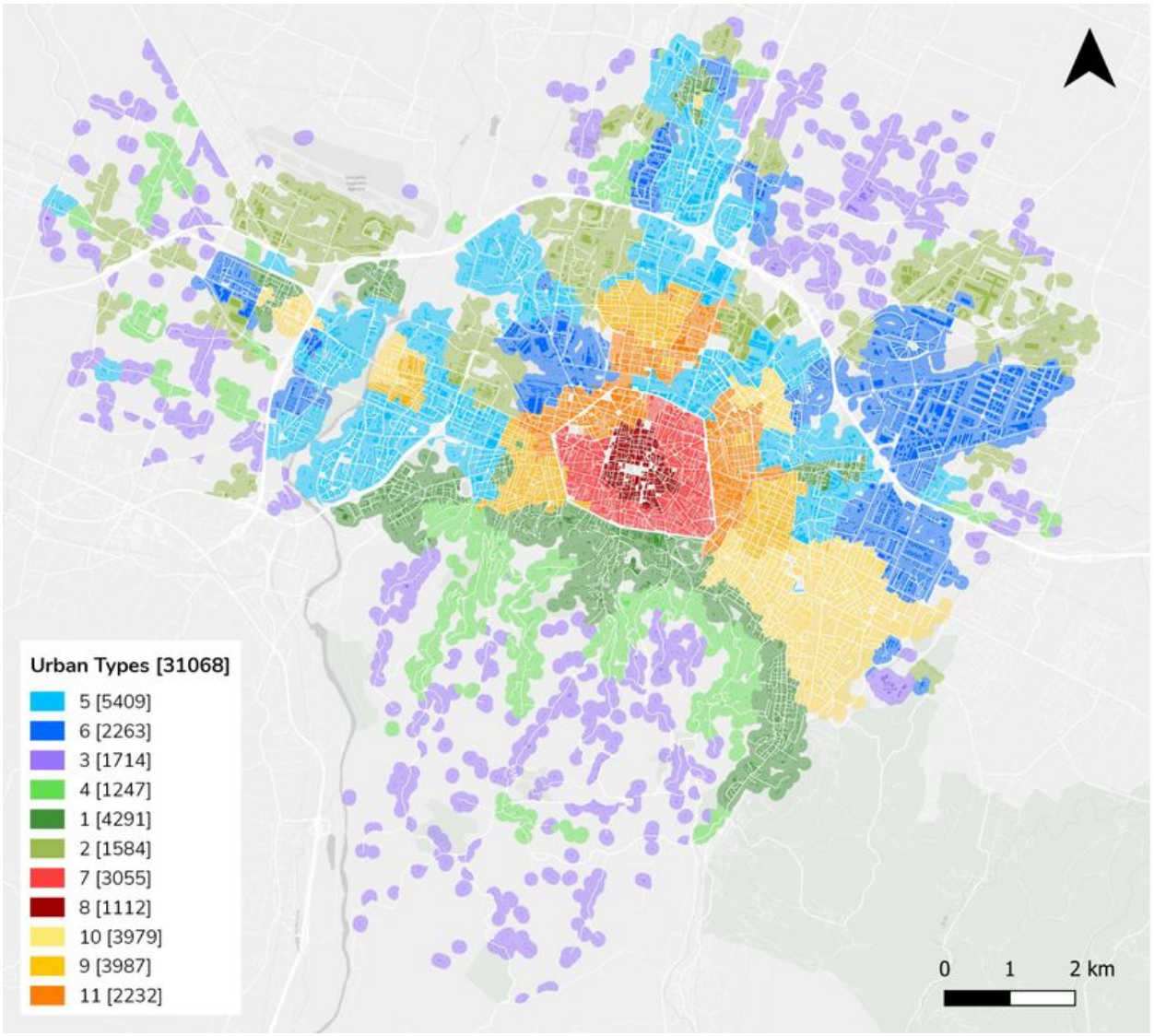

Figure 3
Numerical taxonomy of Bologna (11 UTs): building/cell colors identify UTs. Similarity of colors reflect similarity of form patterns. Source: Authors' own elaboration based on data from Database Topografico Regionale (Regional Topographic Database) of Regione Emilia-Romagna (Emilia-Romagna Region) (2021).

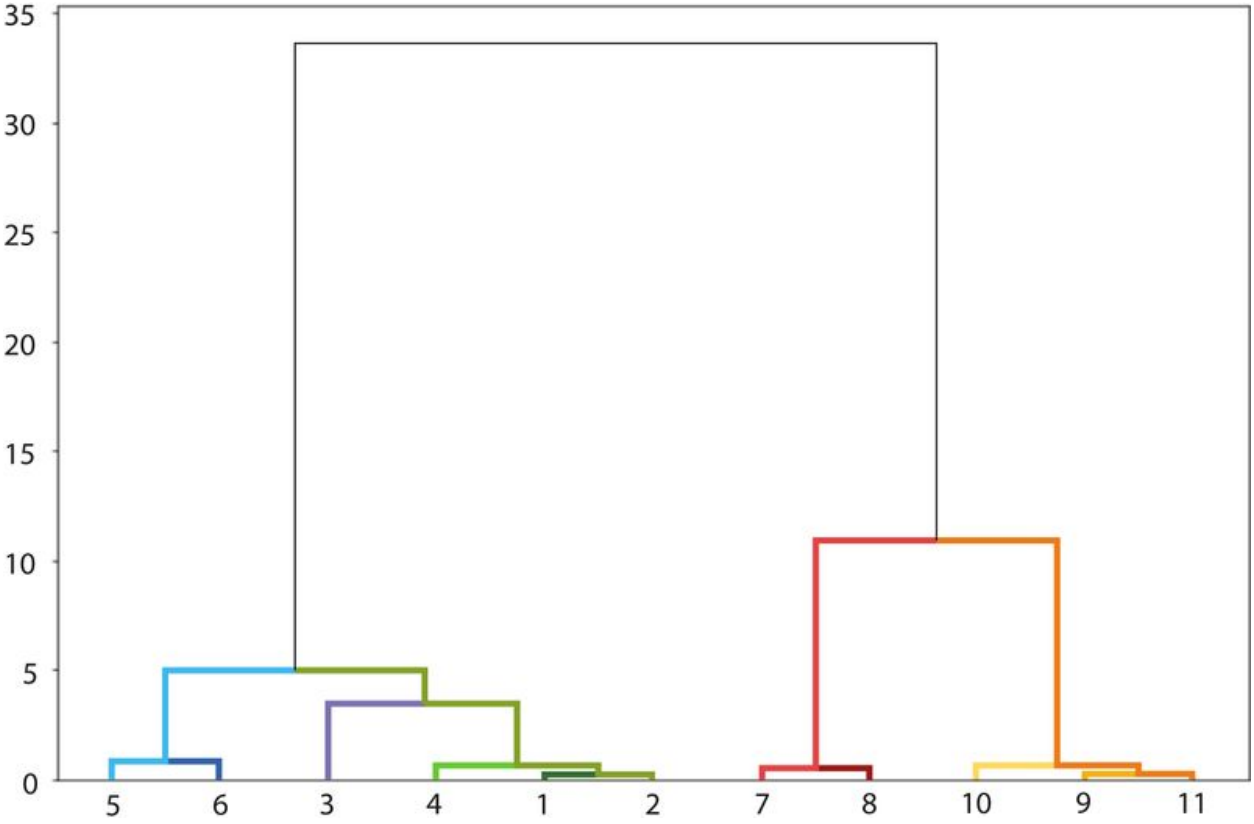

Figure 4
Dendrogram of the 11 UTs of Bologna: similarity between UTs is expressed by both the *y*-value of their point of conjunction (the lower the value, the higher the similarity) and the similarity of their color. Source: Authors' elaboration.

For example, the subbranch of the dendrogram formed by UT7 and UT8 corresponds to the ancient city core and expresses the concentric nature of its development. More specifically, UT8 closely follows the boundaries of the inner fortification wall, the eleventh-century *Cerchia del Torresotti,* which is now largely demolished. This innermost ring features the densest and most ancient urban core originally established in Roman and Etruscan times (Figure 5, top left). In turn, UT7 overlaps with the thirteenth-century circular wall (this, too, now demolished) and matches the later medieval expansion of the city: this is a compact but more porous urban fabric characterized by private and public gardens and small courtyards (Figure 5). Notably, the northwest part of this "rounder" historical core is correctly classified distinctly from UT7 and U8 and, in fact, belongs to UT11. This nicely captures the massive historical alteration of the original medieval pattern implemented after the wider XIX century post-national unification rehabilitation plan (Figure 5, top right). Furthermore, the same area was heavily bombed during World War II and almost entirely redeveloped in the postwar years. Therefore, its urban form is more similar—though

not entirely identical—to that of the first suburban ring developed in the same years (e.g., UT9 and UT10).

UT2 and UT6 also validate the taxonomy. Both are found in peripheral portions of the city and were mostly developed in the second half of the twentieth century. In particular (Figure 5, bottom), UT2 captures most of Bologna's specialist hubs, such as large warehouse complexes (e.g., Bologna International Exhibition Area), airports, military zones, large commercial and productive areas (e.g., Lame Commercial District and Bargellino Industrial District), regional tertiary hubs (e.g., CNR Bologna Research Area), and metropolitan hospitals (e.g., Maggiore Hospital). Analogously, UT6 captures most large-scale social housing estates planned and built according to modernist principles typical of the 1950s and 1960s (Figure 5), such as Villaggio INA Borgo Panigale, Villaggio INA Due Madonne, Barca, Pilastro, Beverara, and Corticella. Interestingly, though remarkably different in terms of function, these two UTs appear to share important similarities in terms of urban form, such as peripheral location, large building footprints, proximity to first-tier road infrastructure, campus-like layout, and extensive (rather than intensive) use of land. Remarkably, however, the taxonomy nicely captures that the two UTs both differ from the more consolidated parts of the city, originating after WWII.

Finally, UT4, UT1, and UT2 all capture a different type of progressively low-density peripheral development, one characterized by small building footprint and, particularly in the case of UT1 and UT4, a more organic pattern that follows the sloping landscape of the Bologna hills.

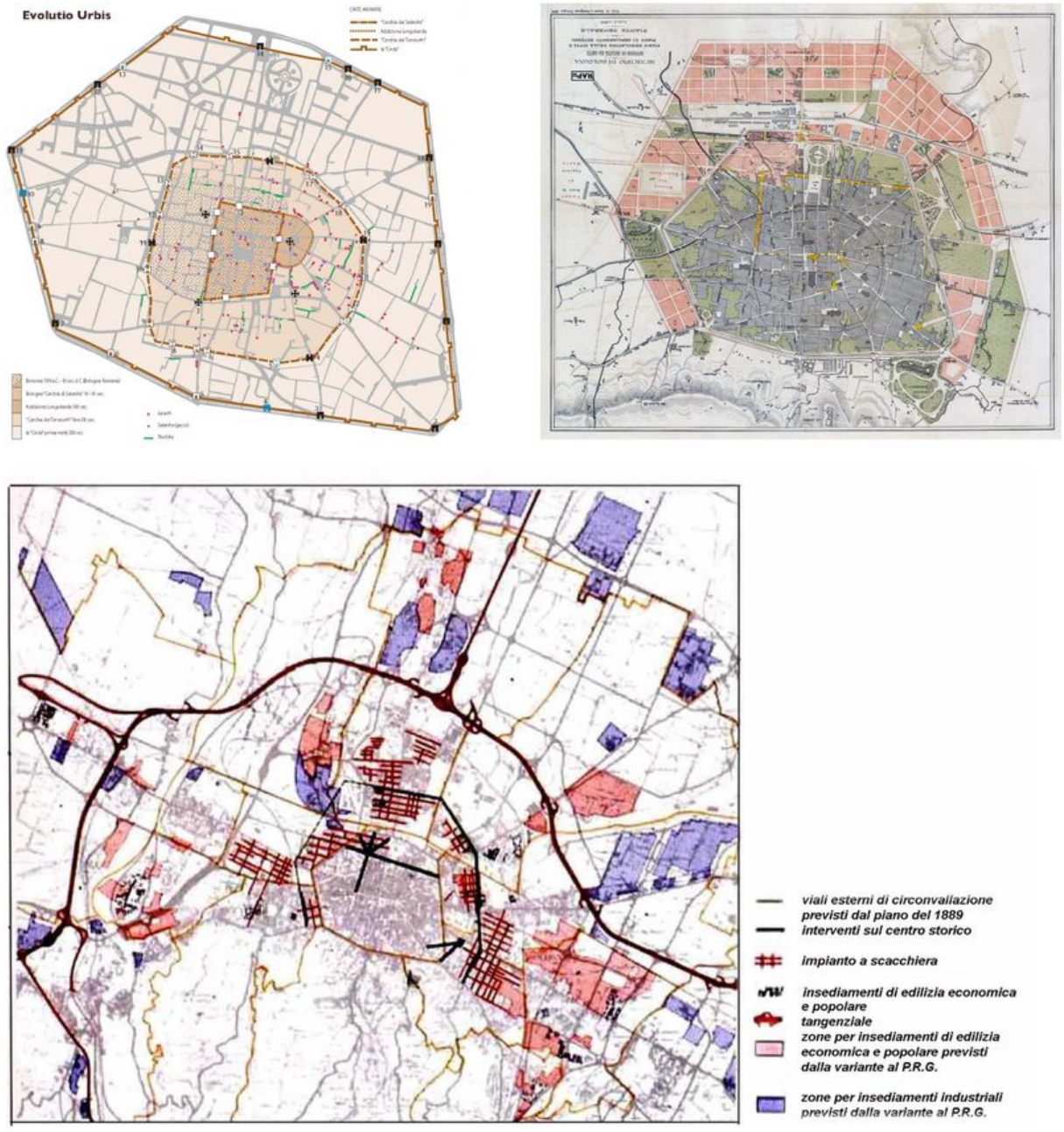

Figure 5
Top left: evolution of Bologna's city walls up medieval times. Top right: first planned expansion of Bologna (1889) outside the XII Century walls (right). Source: website Regione Emilia Romagna. Bottom: planned urban residential and industrial interventions in the periphery of Bologna 1950–1970. Source: Baldeschi, Paolo, and Luciano Anceschi. 1970. *Paesaggio e struttura urbana: aspetti della realtà urbana bolognese*. Bologna, IT: Renana.

The case of Bologna shows that, in urban areas for which quality building and street network data layers are available, UMM is capable of generating a taxonomy rich

enough to capture the subtleties of an urban region's history and functionality that are reflected in the distinctive characters of urban form and that, in this case, were validated against expert, locally produced historic-functional evidence.

What happens when we work in contexts where the quality of the input data is suboptimal? Even when working solely with two widely available data layers, such as buildings and street networks, data consistency and reliability may drop remarkably when the scale of coverage goes beyond the national scale. This is particularly the case when analyzing areas in the Global South in urban contexts characterized by informality, poverty, or unusual environmental conditions. This remains a largely unresolved issue for scientific research, one that prevents implementation of the analysis of urban morphology at extra-large scale unless at enormous cost and/or through a radical reduction of information and/or sampling (Angel et al. 2016; Brelsford et al. 2018; Bettencourt 2020). This problem can be tackled in two ways: 1) by developing the capacity to generate satisfactory results from largely suboptimal input data and 2) by integrating into the workflow the generation of the input data itself, which necessarily involves EO technologies.

These two options are explored in the following section in the city of Kochi, IN, and in the city of Nairobi, KE.

Kochi (IN)

Kochi started as a port city and a key node in the spice and silk trade route. Today, it is a cluster of islands connected to mainland Ernakulam (Liveable Urbanism 2021). The Mattancherry area, where the spice trade originated, has grown informally and organically, with small compact residential buildings and warehouses along the waterfront. To its west is Fort Kochi, more regular, with European influences dating from 1498 onward. Both are culturally and architecturally rich, dotted with historic warehouses, palaces, and civic buildings. The post-independence period (1947 onward) saw the development of dense markets and the expansion of residential neighborhoods inland, in the Ernakulam area. Here, the houses have larger footprints and the urban fabric is less compact, a result of a 1968 Kerala Building Regulation (Government of Kerala 2021) and planned low-income housing. Economic liberalization in the 1990s and large-scale infrastructure development saw the expansion of Kochi further inland and to neighboring islands and villages with commercial and retail developments of high-rises with large footprints on large blocks and the infill of all areas in between as well as ecologically sensitive floodplains around most of the waterfront, which explains the location of fisheries, warehouses, and large undeveloped land.

UMM was applied in Kochi on a largely suboptimal data provision. With no official geographic information available, we explored a database manually created by students of the Masters in Urban Design at the University of Cardiff, UK, between October 2020 and January 2021, including building footprints and the street network. However, we discarded the latter due to inconsistencies in data coverage across the case study area. A common problem in cities in the Global South is that they are dominated by informal urban development, and the street network is very complex. Data repositories (e.g., OpenStreetMap) have very patchy street network data, and in general, the definition of what constitutes a street in the context of an informal area is anything but straightforward (e.g., whether to include internal footpaths or unassigned spaces between buildings). The taxonomy was ultimately generated solely from the building footprint information (Venerandi et al. 2021). Thus, rather than the entire set of 74 primary characters, only 26 were computed (those quantifying dimensions and spatial relations between buildings and cells), resulting in 104 contextual characters. We applied AHC recursively to the latter and identified 24 UTs as optimal.

The resulting taxonomy (Figure 6) proved to be surprisingly significant and still capable of reaching an appreciable degree of accuracy in reflecting morphological periods in the development of the city as embedded in patterns of current urban form. Further explorations conducted in contexts characterized by other kinds of suboptimal data confirmed that, despite the extreme complexity of the factors at play informing the evolution of urban form in time, buildings and streets alone, or even a very partial representation of them, seem sufficient to approximate, to some appreciable degree, the essential patterns of places' distinct identities.

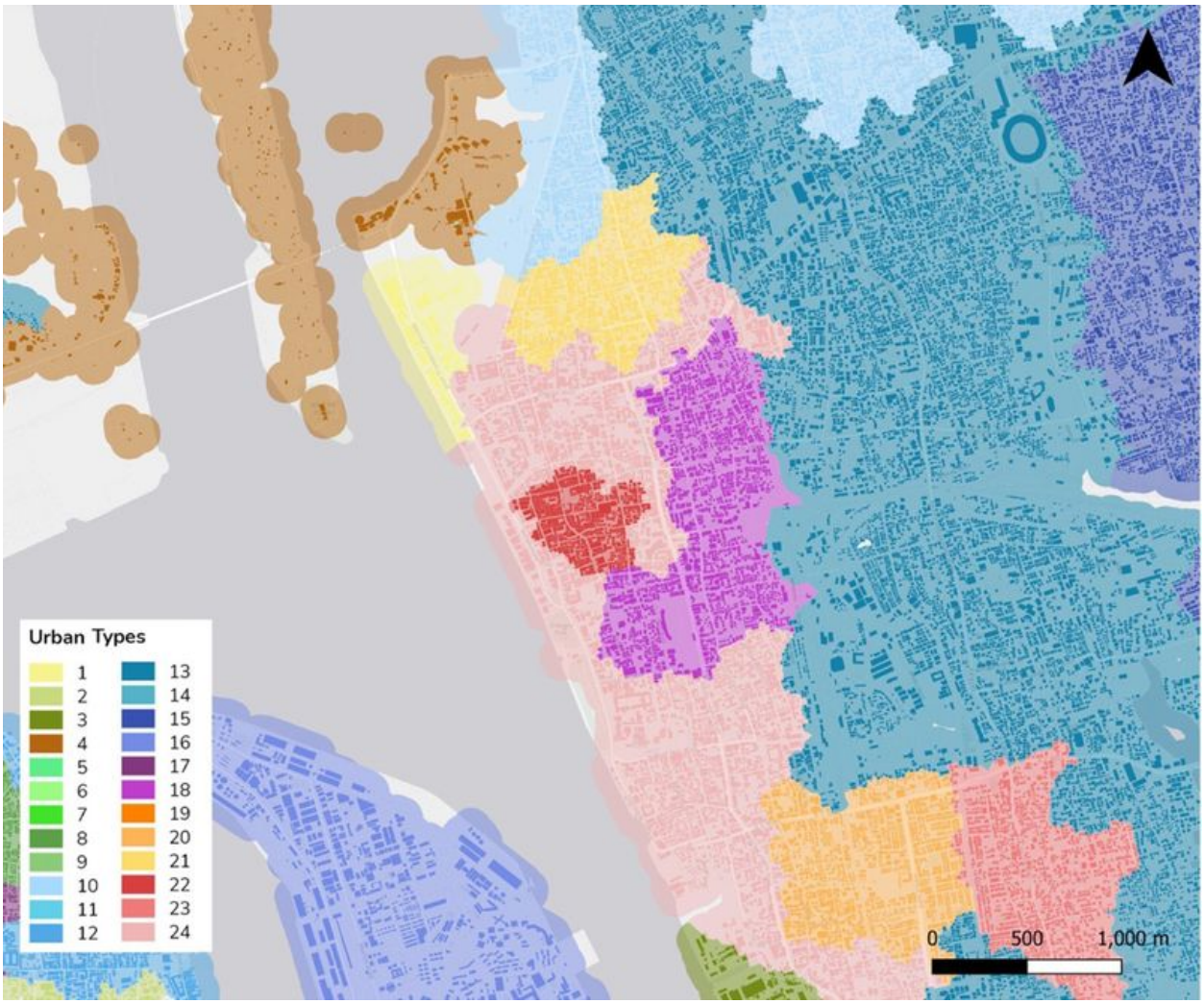

Figure 6
Numerical taxonomy of Kochi (24 UTs), extract centered on the historical Ernakulam market (UT22, red): building/cells' colors identify UTs. Similarity of colors reflect similarity of form patterns. Source: Authors' own elaboration based on data collected from the architecture students at Cardiff University (UK), between October 2020 and January 2021.

Venerandi et al. (2021) explored one further advantage of the UMM method (i.e., the extraction of morphometric profiles for specific UTs: (UT7, UT18 and UT1, subsequent generation of form-based design codes, and potential spinoffs in the area of generative design.

Design Codes (DCs, 2004) are a traditional feature of urban design practice (Hakim 2014) that have known a surge of interest as part of the place-making agenda in the last three decades (Form Based Codes Institute 2004; Parolek, Parolek, and Crawford 2008) and are currently the core of a major reformation of the planning system in the

United Kingdom, the National Model Design Code initiative (Ministry of Housing 2021). Along these lines, UMM opens the way to basing DCs on large-scale evidence extracted from existing UTs in a numerical form. The case of Kochi adds a further dimension of interest to this, since DCs have never been applied in a city developed largely in an informal manner. This section summarizes the rationale of extracting DCs from UMM and using them to generate design proposals in one sample area within UT22, roughly corresponding to the area of the historical Ernakulam market.

While the 24 UTs of Kochi are identified from 26 primary characters, after a review of a range of DC sources and applications, including the UK government's NMDC, we narrowed down the characters to only six: 1) plot size, 2) coverage ratio, 3) building footprint area, 4) building elongation, 5) alignment to surrounding buildings, and 6) distance between buildings (see Table 2 in the Appendix). The selected characters are easy to communicate to designers and stakeholders and, despite the significant reduction of complexity, provide enough indications to inform a preliminary skeleton of figure-grounds.

Starting from the morphometric profile of UT22, we tested the ability of the six characters to inform the (re)generation of a sample area within this UT. As part of the UNICITI "Third Way of Building Asian Cities" 2021 initiative,[2] we engaged a group of professional architects and urban designers to act as final users of the UMM outputs. The designers were instructed to repopulate a sample area in UT22 with newly generated building footprints as if it were completely undeveloped, guided by the intervals of the six selected primary characters included in the morphometric profile (Table 2 in the Appendix). The outputs of such design experiments (Figure 7) seem aligned with the pre-existing "urban character" of UT22, while not being replicas.

In short, the ambition of UMM is to capture numerically the essential spatial structure that brings consistent identity and characters to endless local variations. With this abstract exercise—not to be confused with an actual master plan—we wanted to check to what degree figure-grounds generated by different designers could replicate a pre-existing "urban character" without ever replicating identically its visible form and, importantly, without ever ending up with identical proposals.

Our experiment suggests that UMM-informed DCs—even in the limited version applied in Kochi—have the potential to bring both unity and diversity to the design of places. They have the capacity to inform the generation of a range of design proposals similar in character to the original UT but also somehow different from it as well as from each other in their final layout. This allows professional/user interpretation, adaptation,

accommodation of specific requirements or regulations, and all the complexities of an actual professional process of master planning to unfold, without losing the unique intangible character of a place.

Figure 7
Design proposals for a portion of UT22, corresponding to the area of the historical Ernakulam Market in Kochi. The black dashed line identifies the sample area. Source: Authors' own elaboration based on data collected from the architecture students at Cardiff University (UK), between October 2020 and January 2021.

Since morphometric profiles are provided in ranges of values for each primary descriptor, the potential variations of design outputs are countless, allowing for calibration, personal and collective creativity, adjustment, and co-creation of alternative and appropriate solutions.

The integrated EO perspective and the case of Nairobi (KE)

The two European cases show that UMM can provide accurate quantitative descriptions of urban form in data-rich regions. As we have just seen, UMM also has the potential to be used in urban environments with limited data availability (e.g.,

Kochi) but requires, at least, a consistent building layer. However, in many regions of the world, even building footprint data is not available or, if it is available, it may not cover informal settlements. In this section, we delve deeper into the limitations of current EO techniques for extracting building footprints from satellite imagery, our proposal to tackle such limitations, and its application to the city of Nairobi (KE).

Limitations of current EO techniques

A major obstacle to deriving generalized knowledge of cities through the application of UMM at large scale is the limited availability of consistent building footprint geometry. Although several studies have shown the feasibility of mapping buildings through EO (Liu et al. 2019; Schuegraf and Bittner 2019), they tend to focus on parts of cities rather than entire metropolitan areas, thus having limited scientific validity in terms of reproducibility and generalizability. Google's recently published Open Buildings data set,[3] despite its continental coverage, largely relies on costly high resolution Maxar satellite imagery[4] (i.e., commercial images costing $10,000–20,000 for a large city), which renders its reproducibility extremely expensive (Sirko et al. 2021).

Looking at existing workflows of building mapping, limited reproducibility and generalizability are magnified by issues of model and data unavailability and inconsistency. Many models claim to provide good performance (e.g., the Maxar building footprints); however, they are either insufficiently described or not openly accessible, leading to replicability and accessibility issues. Other models have only been tested with data sets not accessible to the public (e.g., the Microsoft Building Footprints),[5] also limiting reproducibility.

Although convolutional neural networks (CNNs), state-of-the-art artificial intelligence (AI) algorithms, are capable of extracting buildings from imagery by automatically learning a set of representative image features, these learned features vary across cities, or even between places within the same city, due to distinctively different physical patterns of buildings. For instance, a CNN trained with images of formally built areas may be unable to capture building patterns in informally built areas, and a CNN trained with images of specific informal areas is not necessarily able to capture all informal areas, even within the same city (Wang et al. 2019). Thus, experiments validated only on small study areas with desirable but costly imagery data can hardly be generalized to produce consistent building information at large scale.

The proposed EO workflow

To tackle the above limitations, we aim to overcome consistency and availability issues for both data and models. There are many types of free EO based imagery data sets available worldwide (e.g., via the Copernicus Program of ESA); however, requiring consistency with the UMM method narrows the available data sets significantly. Google Earth images and Bing Satellite Maps seem the only options fit for purpose, as they meet the requirement of worldwide coverage. However, we acknowledge that their resolution (0.6–1.2m) is suboptimal for building extraction. We argue that this is a typical trade-off in open science: less desirable but widely available data sets. In this study, we decided to use Google Earth imagery data, as it is more frequently updated than Bing Satellite Maps in urban areas (Lesiv et al. 2018).

The technical workflow to extract buildings from Google Earth images is straightforward: acquiring Google Earth image data for a specific city and extracting building footprints. Google Earth imagery data can be downloaded in multiple ways. Google Earth Pro[6] provides direct image download at the highest resolution. A possible alternative is to use third-party open tools, such as SAS.PLANET, to acquire data from the Google Earth portal.[7] Since our research largely focuses on urban areas, downloading imagery data from Google is not classified as a “mass data download” and thus does not violate any of the data usage guidelines.[8] There are already several studies on the extraction of building footprints or roof outlines from Google Earth images; however, they provided limited discussion on their accuracy or results in informal areas (Xia et al. 2021). Thus, the technical challenge of our research is to improve the accuracy of building footprint mapping in not only formal areas but also informal ones, by using freely available Google Earth images. Recent advancements in CNN architectures for building footprint mapping (Pan et al. 2020) build on encoder-decoder structured CNN architectures, such as the U-Net, and variation in the more detailed structure of the encoder or decoder (allowing diversity in model construction). Therefore, we adopted the U-Net architecture (Ronneberger, Fischer, and Brox 2015) and fine-tuned the detailed structure by replacing the encoder part of the model. The rationale of experimenting with the encoder structure is that representational features at different levels of detail are extracted from this part of the U-Net, which determines its capability to capture the targets. We use part of the pretrained, renowned ResNet-50 as our encoder, as the residual network is good at handling overfitting and vanishing gradient (He et al. 2016). The reason for not using the entire ResNet-50 is that we only wanted to take advantage of the pretrained model to extract lower-level features, so that higher-level features, such as building edges and corners, can be

properly captured from the input images. Thus, once the pretrained part is integrated into the U-Net, the learned low-level features are transferred into the U-Net, and the model must be trained only to learn high-level abstract features, such as rectangular shapes of buildings. Apart from using the freely available Google Earth images, we also relied on an open data repository (the global building data set provided by Wuhan University)[9] to train our model. In general, the availability of training data is a big challenge for urban EO, as training data are often not openly accessible and, when they are, they quickly become obsolete in fast-growing cities. In general, the proposed model works as follows: 1) load Google Earth data; 2) prepare training and test sets; 3) set up the experiment, including model configuration and training; and 4) predict the probability of building presence. For more details, we refer the reader to the full model accessible at https://www.kaggle.com/jonwang4/buildingenome-gpu. The extracted building footprints are raster data showing the probability of pixels belonging to a building footprint. Two further steps, building identification and polygonization, are necessary to extract the buildings and to produce georeferenced vector polygons needed for UMM. The first step produces a binary image, representing buildings and non-buildings. The second step automatically generates building footprints by vectorizing the raster shapes from the previous step. An “orthogonalize” procedure is finally applied to avoid overly irregular shapes

Nairobi (KE)

Nairobi, the capital of Kenya, was founded in the late nineteenth century in conjunction with the railroad development by the British colonial power. The city shows a stark urban divide between well-serviced urban areas and informal settlements. It is estimated that around 60% of its 4.3 million inhabitants live in informal settlements on around 6% of the built-up areas (leading to very high built-up densities) (Wamukoya et al. 2020). The city is strongly divided between well-serviced urban areas and informal settlements. This urban divide goes back to the British colonial history and the long-standing effects of residential racial zoning. More recently, the city was divided into European and Asian zones (Maganga 2021). The former is characterized by low coverage area ratio (around 50%) and is located in higher and thus less flood-prone lands, in the northwest of the city. The latter is located around the CBD and the industrial areas in the northeast. The low-lying eastern region and areas alongside main infrastructures (e.g., railroads) have been rapidly developing, in particular after independence in 1963. The rapid increase of Nairobi’s population combined with the low supply of low-income housing has led to the massive growth of informal areas (Gatabaki-Kamau and Karirah-Gitau 2004).

By applying the EO workflow presented above to the Google Earth images covering the entire city (roughly 20 GB of data), we obtained 506,435 building footprints (Figure 8). Through visual inspection, we observe a considerable morphological heterogeneity, with dense areas intermingled with more dispersed ones. By zooming in further (Figure 9), results show that buildings in very dense parts can be captured (Figure 9, right frame), including those in extremely dense informal areas (Figure 8, middle frame). Outputs seem to hold also in more dispersed/rural contexts (Figure 9, left frame). However, several incorrect predictions can be found in the northwestern corner of the study area (Figure 9, right frame), where rectangular bare crop parcels are predicted as buildings. These are very similar to building roofs in terms of shape, color, and texture; thus, our method, which uses RGB images as input, struggles to differentiate them from buildings.

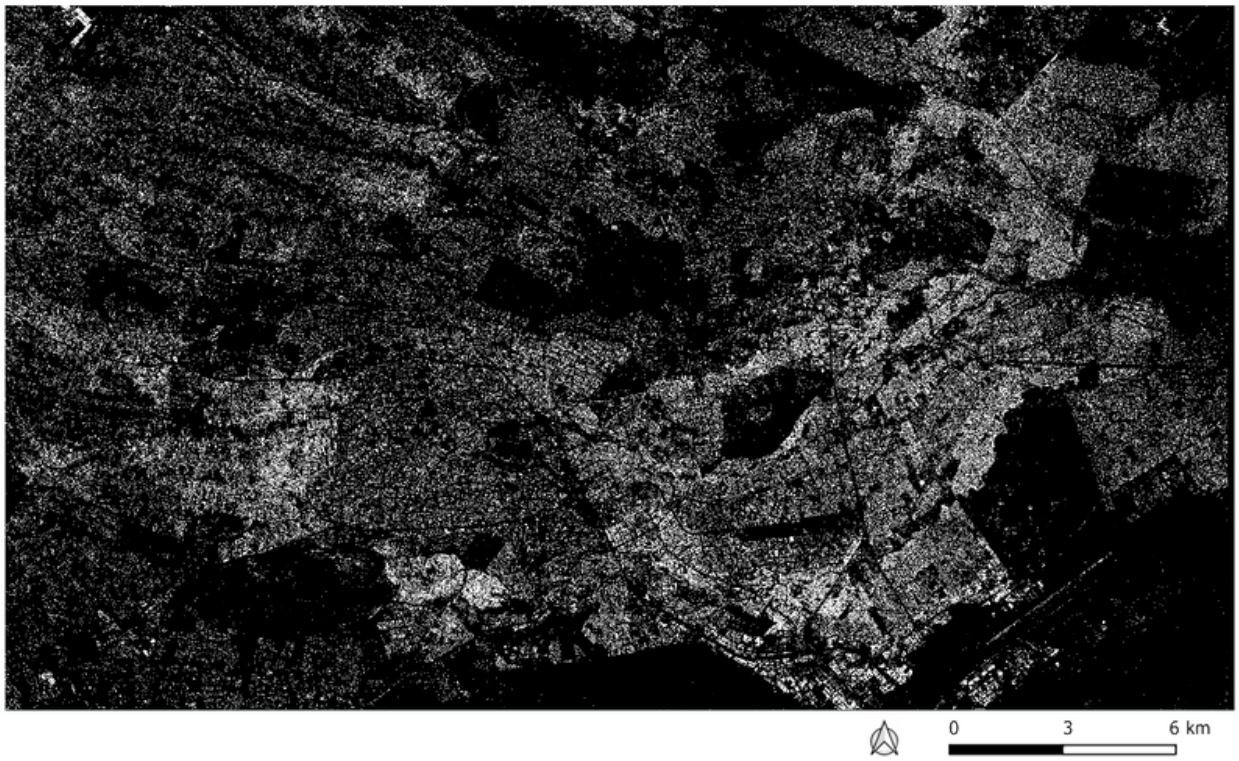

Figure 8
Building footprints of Nairobi, Kenya, extracted through the proposed EO workflow. Source: Authors' elaboration.

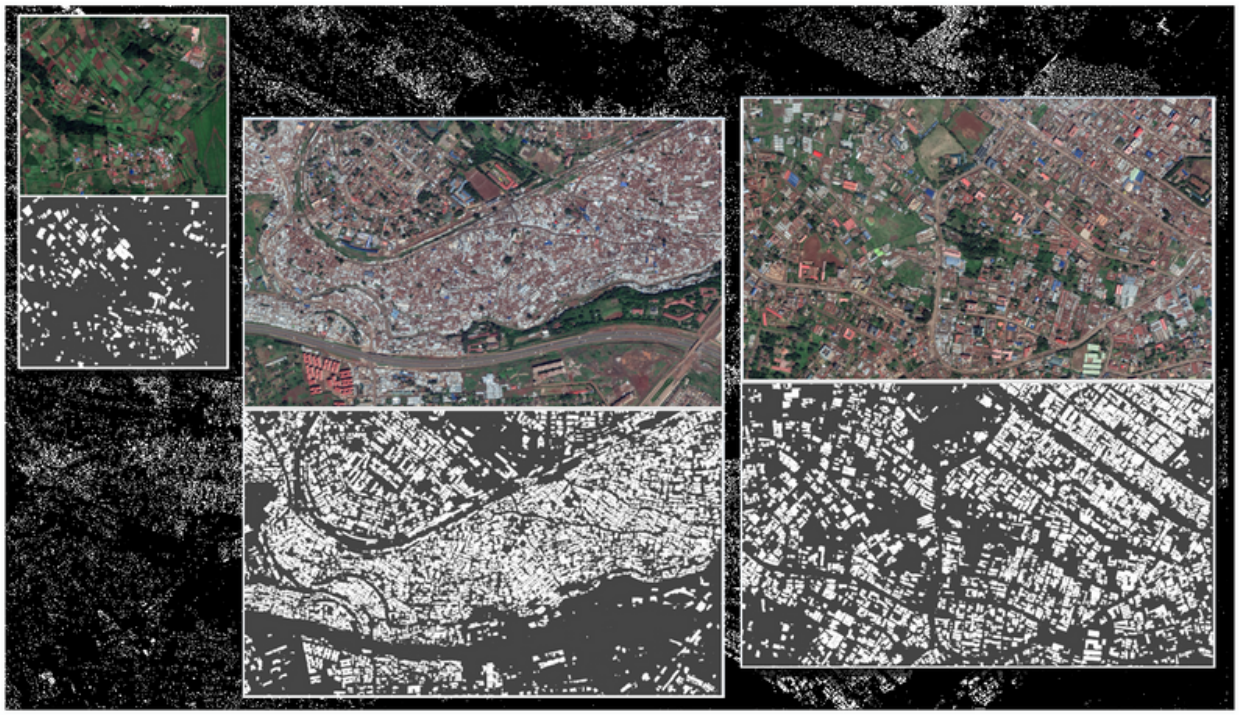

Figure 9
Map extracts of building footprints in Nairobi. Left: dispersed/rural setting. Middle: dense informal area. Right: dense area with bare crop parcels. Source: Author(s)'s elaboration and Google Earth.

To validate results, we focus on a heterogeneous area of Nairobi (mixing industrial, informal and formal fabrics) and visually compare the satellite Google Earth image (Figure 10a) and manually drawn buildings (Figure 10b) with Google AI Open Buildings using paid Maxar Technologies (CNES/Airbus) (Sirko et al. 2021) (Figure 10c), OSM buildings[10] (Figure 10d), and buildings extracted from free images through our proposed EO workflow (Figure 10e). We observe the following:

- In terms of data coverage, both Google's (c) and our (e) extracted footprints cover a significant part of the existing buildings, as portrayed in the satellite image (a) and the manually drawn buildings (b). On the other hand, OSM's coverage is very limited.
- In terms of footprint shape, both our and Google's automatically extracted outlines generally underestimate the size of building footprints.
- In terms of granularity, our extraction seems to better reflect the actual condition on the ground, as represented in both satellite (a) and manually drawn representations (b). Google's buildings, in some instances, tend to be larger than they should, as several small adjacent buildings are not accounted for. For comparison, see the bottom left of (c) and (e).

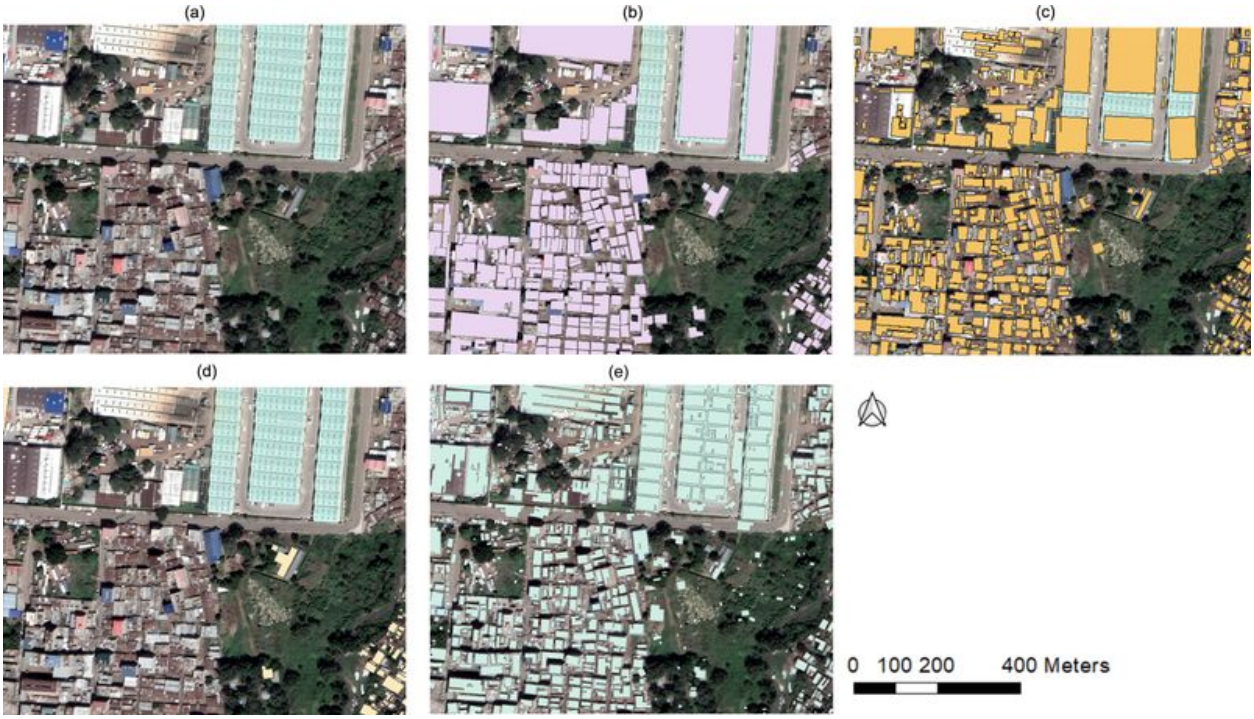

Figure 10
Validation of the building footprints extracted through the proposed EO workflow. (a) Original Google Earth image. Source: Google Earth. (b) Manually drawn building footprints. Source: Author(s)'s elaboration and Google Earth. (c) The Google AI Open Buildings from paid Maxar Technologies, CNES/Airbus. Source: Sirko et al . (2021) and Google Earth. (d) The OSM building layer. Source: OSM contributors and Google Earth. (e) Polygonized building footprints with further orthogonal corrections. Source: Author(s)'s elaboration and Google Earth.

Although the building footprints extracted through the proposed EO workflow are suboptimal, we nevertheless used them as input for the UMM method to understand to what extent the latter tolerates inaccuracies as a compromise of using an open data source. To do so, we applied the UMM method to both the manually drawn and automatically extracted data presented above. As in Kochi, only 26 of the original 74 primary characters are computed, and thus only 104 of the original 296 contextual characters are derived for both data sets. AHC is then recursively applied to the 104 contextual characters to test solutions drawn from 2–10 UTs. The silhouette score is then used to identify the optimal number for each data set (see Figure 12, in the Appendix). Figure 11 shows the results of the clustering for both manually drawn (left) and automatically extracted (right) building footprints. The optimal numbers of UTs were found to be five in the manually drawn and seven in the automatically extracted. It is possible to remark that, even with suboptimal data, the observed morphological patterns appear similar for the two data sources. In both cases, buildings belonging to the informal part in the center of the sample area are properly classified in a dedicated

UT (i.e., UT0). A minor issue concerns the UT0 computed from the automatically extracted buildings, as it also incorporates the southwestern part of the sample area, which might not be fully informal. The noise obtained from the suboptimal data is largely classified in a distinct cluster (UT3 in Figure 11, right), thus not significantly impacting the classification of the existing urban form.

In this section, we illustrated how the proposed EO workflow can extract building footprints from available satellite imagery (i.e., Google Earth). Although the extracted data is found to be suboptimal, preliminary results show that it can still be used in UMM to obtain morphologically significant descriptions.

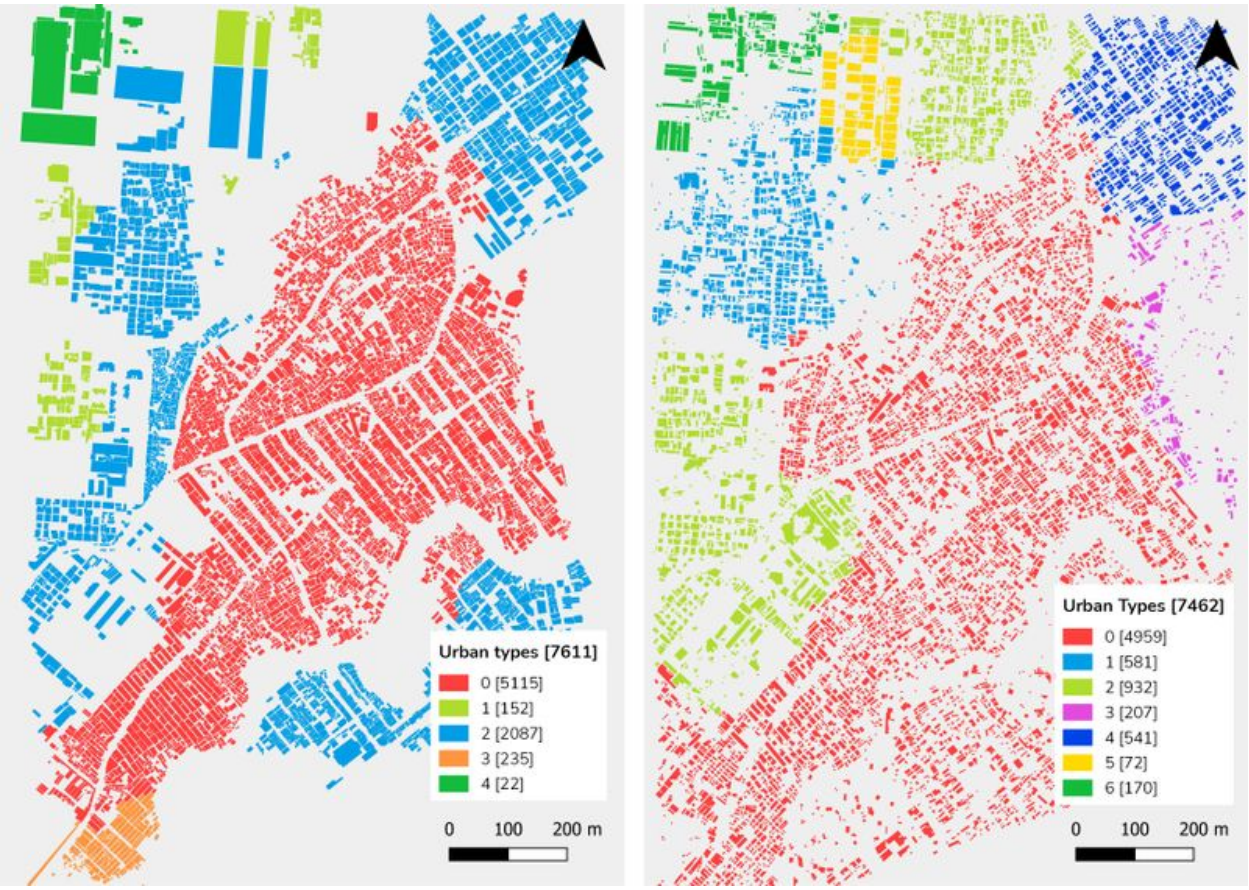

Figure 11
Numerical taxonomy of a sample area in Nairobi, KE; UTs generated through the UMM method from manually drawn (left) and automatically extracted (right) building footprints. Source: Author(s)'s elaboration.

Discussion

Illustrated on two European cases (Amsterdam and Bologna), we showed that the UMM method allows the identification of UTs that meaningfully reflect the urban morphology of the cities under examination. In general, UMM requires consistent building footprints and street network data that are typically available in the Global North but are often lacking in the Global South. Therefore, we used an example from the Global South (Kochi) to test whether building footprints were sufficient for UMM. The results presented in this work confirmed that they were. However, in most cities of the Global South, access to consistent and up-to-date spatial data on buildings is a challenge. We thus created a composite EO/machine learning technique able to automatically extract building footprints from openly accessible satellite imagery. The application of the UMM method to building footprints extracted for a sample area in Nairobi confirms the potential of combining EO and UMM in an integrated and replicable workflow able to identify distinctive morphological patterns.

This new avenue solves a significant challenge that has hindered global morphometric analysis, allowing the generation of a geography of urban form that is unprecedented in terms of scale of extent and richness of information. From the point of view of fundamental research, this new geography paves the way for the initiation of a proper, systematic science of urban form evolution, which departs from traditional analogies between cities and living organisms to approach this relation at an ontological level, recognizing biological and urban form systems as both complex and adaptive. From the point of view of the potential of this new geography in terms of its immediate application, four areas are considered, which currently are under exploration. (1) Urban policy support: this is the extent to which urban form contributes to the socioeconomic and environmental performance of cities and communities has always been built on qualitative information often generated from limited scale case studies or personal observations. By providing a comprehensive numerical description of urban form, UMM allows the integration of morphological analysis into the wider area of urban analytics. This, in turn, opens up a systematic and replicable large-scale observation of the relationship between urban form and virtually any available data on urban life, such as deprivation, health, prosperity, mobility, or carbon footprint. (2) Urban design regulation and codes: UMM paves the way for evidence-based coding policies, in which specifications proposed for new interventions (new developments as well as regeneration) are based on numerical urban form identities detected from existing urban places. (3) Effecting urban engagement strategies: large-scale/rich numerical information on urban form supports innovative tools for generative design

approaches aimed at the engagement of industry, stakeholders, and local communities in co-creating solutions for cities. Morphometric dashboards may enact gaming routines based on actual urban data, including urban form, in the framework of multiactorial modeling interactions. (4) Morphological indicators on the diversity of urban form link to urban sustainability: for example, the urban SDG indicator 11.1.1 mainly uses a binary classification of slum/non-slum areas, while the results of the integrated approach shown here suggest the physical diversity of such areas, which can be related to other sustainability indicators (e.g., health, hazards, climate change). Furthermore, such an analysis is also relevant for low-income housing areas that might not be reported under SDG 11.1.1 and can guide the identification of local actions and interventions.

In this paper, we illustrated how the UTs observed in the case studies show resemblances to existing city patterns and stages of urban development. However, further systematic validations are needed. These may include, for example, correlational studies with various socioeconomic, environmental, land use, and well-being data. These will not only ensure more robust grounding to UMM but also provide further insights on cities and overall urbanization patterns. Further investigations should also focus on comparing UMM outputs obtained with optimal (buildings with heights and street network) and suboptimal (buildings-only) data. While the latter scenario is, to a certain extent, disadvantageous for the generation of DCs, as street features cannot be included, it could, nevertheless, be relevant for generating taxonomies in a faster manner and with less input data. Finally, we note that UMM is not designed to output a fixed/optimal number of UTs. Since one of the main aims of the methodology is scalability, having a fixed number of UTs over extra-large spatial extents would make the description at the local scale too coarse for planning and urban design purposes. In this paper, the silhouette diagram is used to identify the number of UTs at the city scale, but future work will investigate methods to interactively “scroll up and down” the complete dendrogram at users’ discretion, to obtain visualizations of different numbers of UTs according to scale, while keeping the dendrogram’s structure and the quality of the resulting taxonomies unaltered.

Acknowledgements

This work was supported by the Axel and Margaret Ax:son Johnson Foundation as part of “The Urban Form Resilience Project” at the University of Strathclyde.

We are very grateful to the UNICITI's founder and director Olga Chepelianskaia and volunteer professional designers Kavya Kalyan, Vija Viese, Nitin Bhardwaj, and Sebastián Ugás for helping with the design (re)generation starting from the morphometric profiles of UTs.

Our gratitude also goes to Martin Fleischmann and Nick Bristow. Martin worked out the Nairobi case study characters' calculation as part of an ongoing research collaboration and amicably reviewed this paper internally vis-à-vis external peer reviewers. Nick very kindly and competently edited the English language.

Appendix

character	element	scale	context	category
area	building	S	building	dimension
height	building	S	building	dimension
volume	building	S	building	dimension
perimeter	building	S	building	dimension
courtyard area	building	S	building	dimension
form factor	building	S	building	shape
volume to façade ratio	building	S	building	shape
circular compactness	building	S	building	shape
corners	building	S	building	shape
squareness	building	S	building	shape
equivalent rectangular index	building	S	building	shape
elongation	building	S	building	shape

Centroid—corner distance deviation	building	S	building	shape
Centroid—corner mean distance	building	S	building	shape
solar orientation	building	S	building	distribution
street alignment	building	S	building	distribution
cell alignment	building	S	building	distribution
longest axis length	tessellation cell	S	tessellation cell	dimension
area	tessellation cell	S	tessellation cell	dimension
circular compactness	tessellation cell	S	tessellation cell	shape
equivalent rectangular index	tessellation cell	S	tessellation cell	shape
solar orientation	tessellation cell	S	tessellation cell	distribution
street alignment	tessellation cell	S	tessellation cell	distribution
coverage area ratio	tessellation cell	S	tessellation cell	intensity
floor area ratio	tessellation cell	S	tessellation cell	intensity
length	street segment	S	street segment	dimension
width	street profile	S	street segment	dimension
height	street profile	S	street segment	dimension
Height-to-width ratio	street profile	S	street segment	shape
openness	street profile	S	street segment	distribution

width deviation	street profile	S	street segment	diversity
height deviation	street profile	S	street segment	diversity
linearity	street segment	S	street segment	shape
area covered	street segment	S	street segment	dimension
buildings per meter	street segment	S	street segment	intensity
area covered	street node	S	street node	dimension
shared walls ratio	adjacent buildings	M	adjacent buildings	distribution
alignment	neighboring buildings	M	neighboring cells (queen)	distribution
mean distance	neighboring buildings	M	neighboring cells (queen)	distribution
weighted neighbors	tessellation cell	M	neighboring cells (queen)	distribution
area covered	neighboring cells	M	neighboring cells (queen)	dimension
reached cells	neighboring segments	M	neighboring segments	intensity
reached area	neighboring segments	M	neighboring segments	dimension
degree	street node	M	neighboring nodes	distribution
mean distance to neighboring nodes	street node	M	neighboring nodes	dimension
reached cells	neighboring nodes	M	neighboring nodes	intensity

reached area	neighboring nodes	M	neighboring nodes	dimension
number of courtyards	adjacent buildings	L	joined buildings	intensity
perimeter wall length	adjacent buildings	L	joined buildings	dimension
mean interbuilding distance	neighboring buildings	L	cell queen neighbors 3	distribution
building adjacency	neighboring buildings	L	cell queen neighbors 3	distribution
gross floor area ratio	neighboring tessellation cells	L	cell queen neighbors 3	intensity
weighted reached blocks	neighboring tessellation cells	L	cell queen neighbors 3	intensity
area	block	L	block	dimension
perimeter	block	L	block	dimension
circular compactness	block	L	block	shape
equivalent rectangular index	block	L	block	shape
compactness-weighted axis	block	L	block	shape
solar orientation	block	L	block	distribution
weighted neighbors	block	L	block	distribution
weighted cells	block	L	block	intensity
local meshedness	street network	L	nodes 5 steps	connectivity

mean segment length	street network	L	segment 3 steps	dimension
cul-de-sac length	street network	L	nodes 3 steps	dimension
reached cells	street network	L	segment 3 steps	dimension
node density	street network	L	nodes 5 steps	intensity
reached cells	street network	L	nodes 3 steps	dimension
reached area	street network	L	nodes 3 steps	dimension
proportion of cul-de-sacs	street network	L	nodes 5 steps	connectivity
proportion of three-way intersections	street network	L	nodes 5 steps	connectivity
proportion of four-way intersections	street network	L	nodes 5 steps	connectivity
weighted node density	street network	L	node	intensity
local closeness centrality	street network	L	nodes 5 steps	connectivity
square clustering	street network	L	nodes within network	connectivity

Table 1. List of the 74 primary characters, alongside spatial element, scale, spatial context and conceptual category. Formulas can be found in (Fleischmann et al. 2021b)

Interval plot size	% plot size	Interval coverage ratio	% coverage ratio	Interval building footprint	% building footprint	Interval building elongation	% building elongation	Interval alignment surrounding buildings	% alignment surrounding buildings	Interval mean distance between buildings	% mean distance between buildings
(36.59, 336.09)	58.0693816	(0.03, 0.06)	0.15082956 26	(5.11, 78.95)	16.4404223 2	(0.07, 0.20)	2.26244343 9	(0.27, 1.43)	15.3846153 8	(0.36, 3.67)	39.0648567 1
(336.09, 650.88)	28.0542986 4	(0.06, 0.11)	0.15082956 26	(78.95, 145.13)	29.2609351 4	(0.20, 0.31)	6.63650075 4	(1.43, 2.31)	26.5460030 2	(3.67, 5.95)	34.0874811 5
(650.88, 1080.39)	10.2564102 6	(0.11, 0.16)	0.90497737 56	(145.13, 234.55)	23.5294117 6	(0.31, 0.39)	8.14479638	(2.31, 3.12)	19.7586727	(5.95, 8.33)	18.7028657 6
(1,080.39, 1677.60)	2.56410256 4	(0.16, 0.20)	0.90497737 56	(234.55, 371.63)	15.9879336 3	(0.39, 0.46)	9.04977375 6	(3.12, 3.95)	15.8371040 7	(8.33, 10.96)	4.67571644
(1,677.60, 2515.36)	0.75414781 3	(0.20, 0.25)	1.35746606 3	(371.63, 585.08)	9.04977375 6	(0.46, 0.52)	7.39064856 7	(3.95, 4.83)	7.84313725 5	(10.96, 13.91)	1.8095475 1
(2,515.36, 3689.55)	0.15082956 26	(0.25, 0.29)	1.05580693 8	(585.08, 910.02)	4.07239819	(0.52, 0.57)	10.2564102 6	(4.83, 5.78)	5.12820512 8	(13.91, 17.34)	0.75414781 3

(3,689.55, 5266.39)	0.15082956 26	(0.29, 0.33)	3.167420814	(910.02, 1430.61)	1.055806938	(0.57, 0.62)	7.239819005	(5.78, 6.84)	4.37405731 5	(17.34, 21.52)	0.60331825 04
(5,266.39, 7385.03)	0	(0.33, 0.38)	4.072 39819	(1,430.61, 2212.47)	0.452 4886878	(0.62, 0.66)	6.787 330317	(6.84, 8.06)	1.960 784314	(21.52, 26.72)	0.301 6591252
(7,385.03, 10,282.65)	0	(0.38, 0.42)	4.072 39819	(2,212.47, 3423.68)	0	(0.66, 0.71)	5.580 693816	(8.06, 9.53)	1.508 295626	(26.72, 33.26)	0
(10,282.65, 14,106.60)	0	(0.42, 0.47)	7.088 989442	(3,423.68, 5308.78)	0.150 8295626	(0.71, 0.75)	7.239 819005	(9.53, 11.39)	0.904 9773756	(33.26, 41.53)	0
(14,106.60, 19,523.60)	0	(0.47, 0.51)	7.692 307692	(5,308.78, 7792.22)	0	(0.75, 0.80)	6.938 159879	(11.39, 13.81)	0.452 4886878	(41.53, 52.31)	0
(19,523.60, 26,922.44)	0	(0.51, 0.56)	12.21 719457	(7,792.22, 10,715.89)	0	(0.80, 0.85)	5.128 205128	(13.81, 17.03)	0.150 8295626	(52.31, 67.13)	0
(26,922.44, 35,608.03)	0	(0.56, 0.63)	16.59 125189	(10,715.89, 14,611.60)	0	(0.85, 0.90)	6.184 012066	(17.03, 21.37)	0.150 8295626	(67.13, 87.98)	0
(35,608.03, 48,659.49)	0	(0.63, 0.71)	20.51 282051	(14,611.60, 26,037.39)	0	(0.90, 0.95)	5.580 693816	(21.37, 27.66)	0	(87.98, 118.10)	0

(48,659.49, 67,909.16)	0	(0.71, 1.34)	20.060331833	(26,037.39, 34,898.16)	0	(0.95, 1.00)	5.5806938116	(27.66, 40.37)	0	(118.10, 199.79)	0
Table 2. Morphometric profile of UT22											

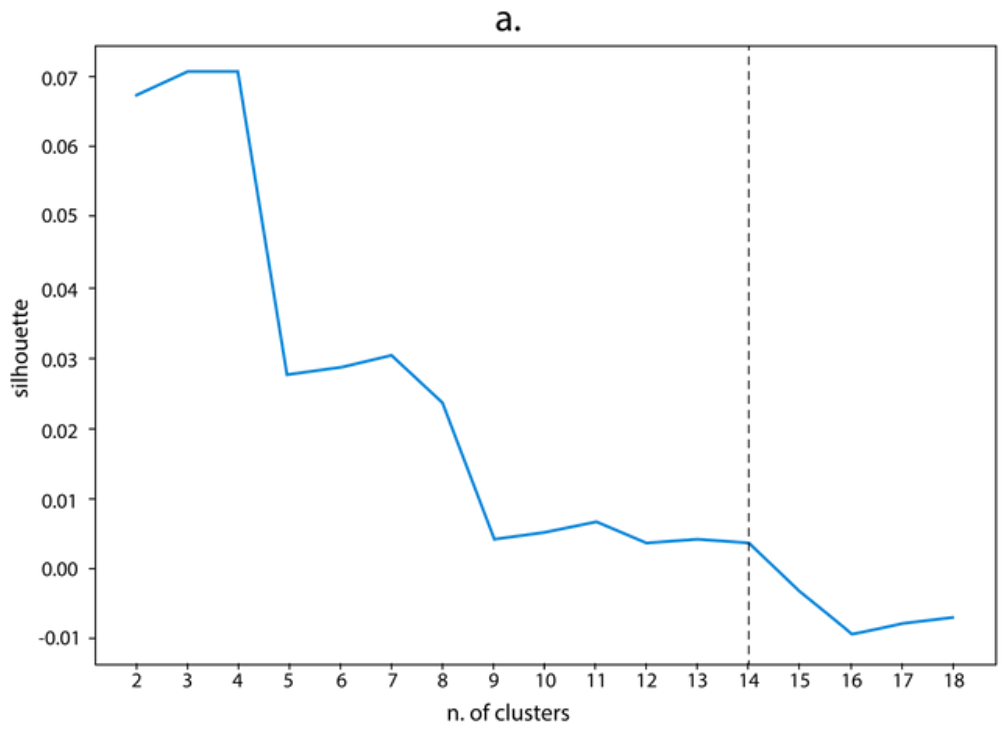

Figure 12
(a.) Amsterdam;

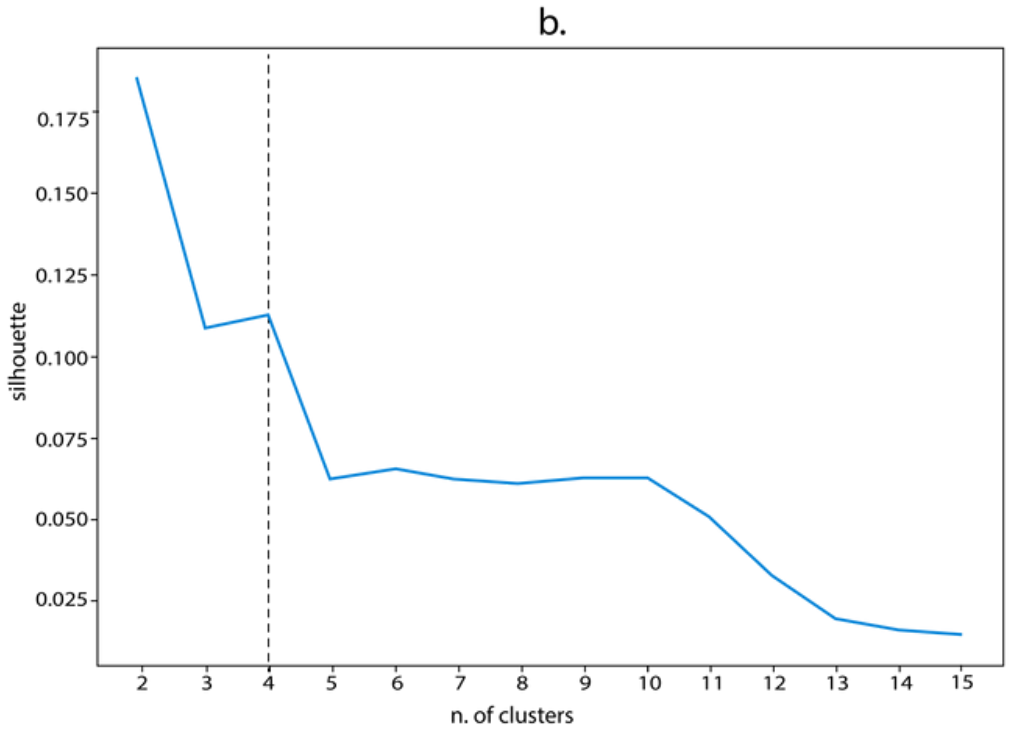
b.
silhouette
0.175
0.150
0.125
0.100
0.075
0.050
0.025
2
3
4
5
6
7
8
9
10
11
12
13
14
15
n. of clusters

Figure 13

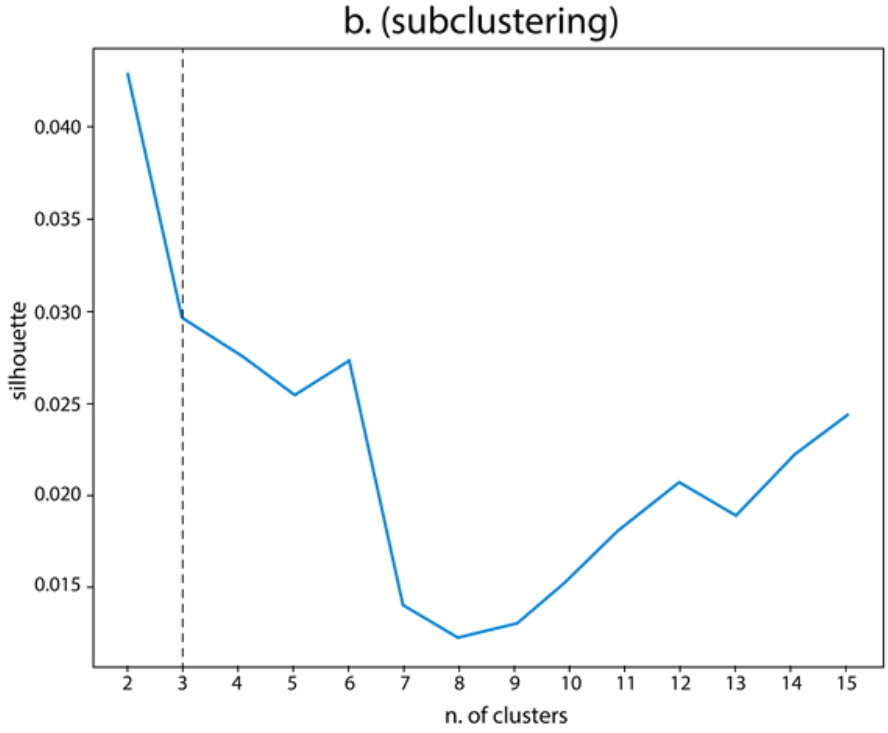
b. (subclustering)
silhouette
0.040
0.035
0.030
0.025
0.020
0.015
2
3
4
5
6
7
8
9
10
11
12
13
14
15
n. of clusters

Figure 14

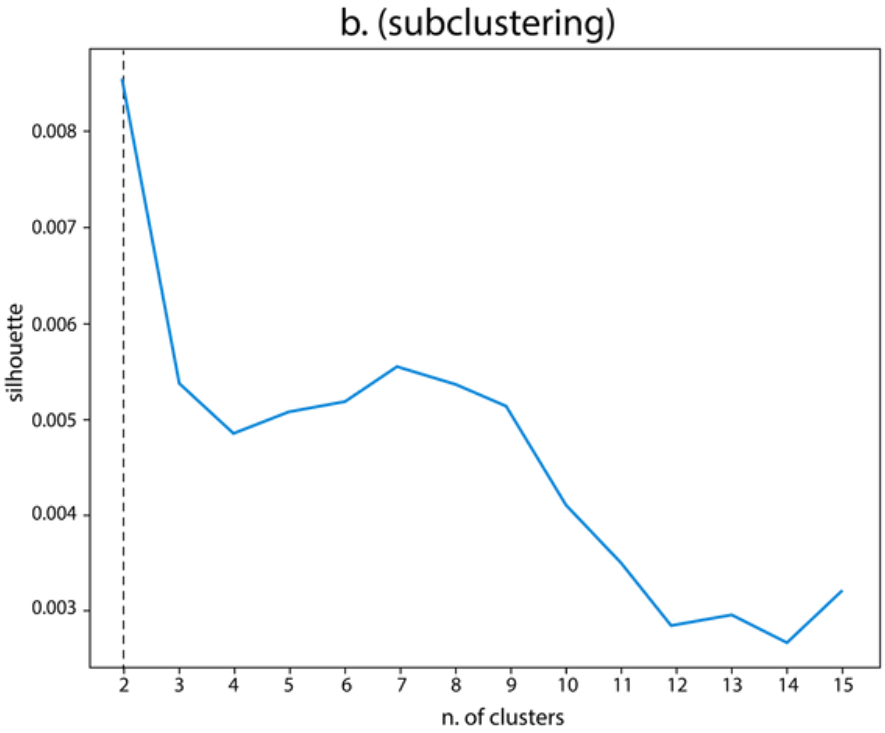
b. (subclustering)
silhouette
0.008
0.007
0.006
0.005
0.004
0.003
2
3
4
5
6
7
8
9
10
11
12
13
14
15
n. of clusters

Figure 15

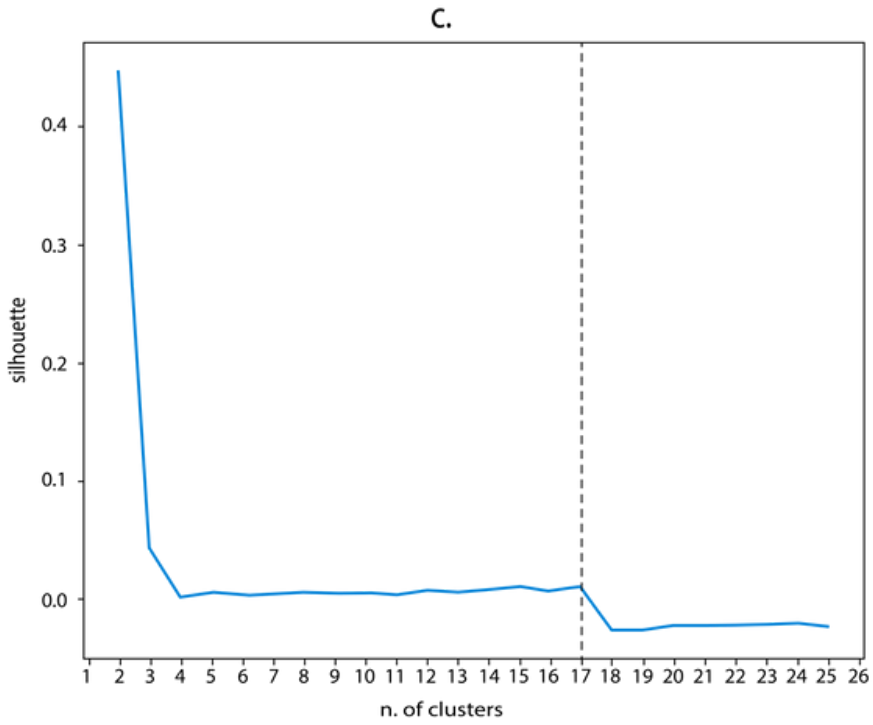
C.
silhouette
0.4
0.3
0.2
0.1
0.0
1 2 3 4 5 6 7 8 9 10 11 12 13 14 15 16 17 18 19 20 21 22 23 24 25 26
n. of clusters

Figure 16

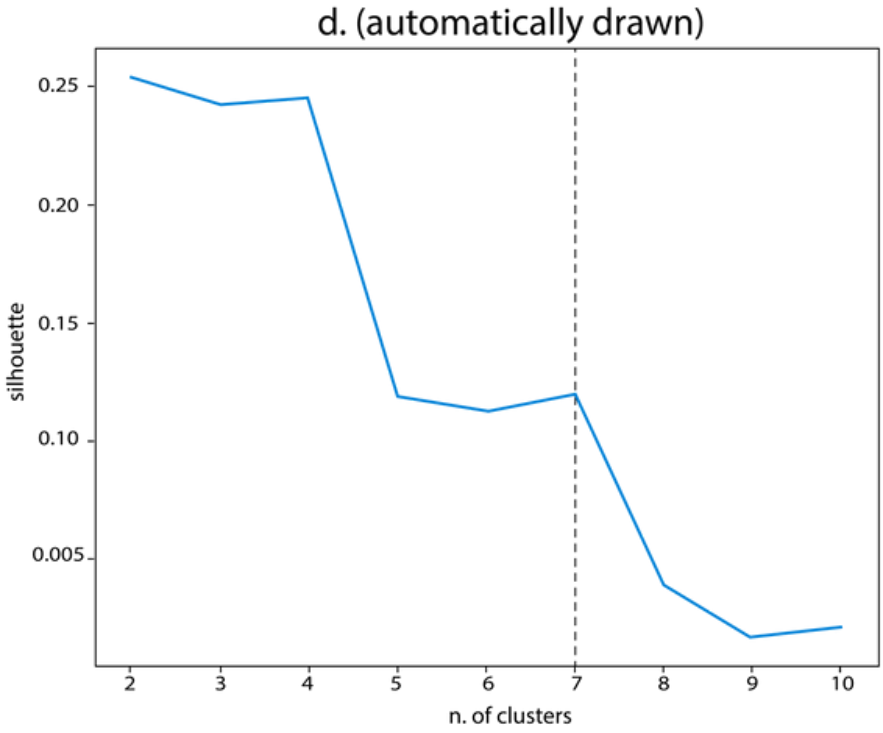
d. (automatically drawn)
silhouette
0.25
0.20
0.15
0.10
0.005
2
3
4
5
6
7
8
9
10
n. of clusters

Figure 17

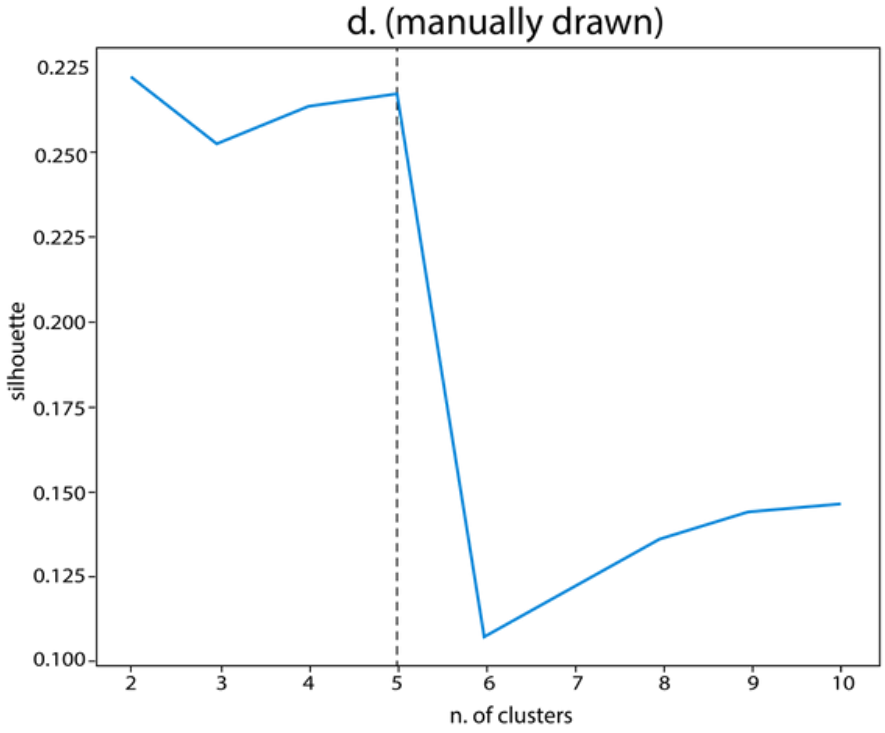

Figure 18

Figure 12: Silhouette diagrams for the case studies under examination: (a) Amsterdam; (b.) Bologna; (c.) Kochi; (d.) sample area in Nairobi.

Footnotes

1. https://geoportale.regione.emilia-romagna.it/ ↩
2. https://doha2020.isocarp.org/paper-platform/abstract/public/209/building-unique-cities-a-paradigm-shift-in-the-global-south ↩
3. https://sites.research.google/open-buildings/ ↩
4. Maxar Building Footprints: https://blog.maxar.com/earth-intelligence/2018/gis-ready-building-footprint-shapefiles-for-accelerated-analysis ↩
5. Microsoft Building Footprints: https://www.microsoft.com/en-us/maps/building-footprints ↩
6. https://www.google.com/earth/versions/ ↩

7. http://www.sasgis.org/sasplaneta/ ↩
8. https://www.google.com/permissions/geoguidelines/ ↩
9. http://gpcv.whu.edu.cn/data/building_dataset.html ↩
10. https://wiki.openstreetmap.org/wiki/Buildings ↩

Citations

- Angel, S., P. Lamson-Hall, M. Madrid, A. M. Blei, J. Parent, Sanchez N. Galarza, and K. Thom. 2016. *Atlas of Urban Expansion—2016 Edition: Blocks and Roads*. Vol. 2. New York, Nairobi, Cambridge, MA: NYU Urban Expansion Program at New York University, UN-Habitat, and the Lincoln Institute of Land Policy.

  ↩
- Bettencourt, Luis. 2020. “Million Neighbourhoods.” Mansueto Iinstitte for Urban Innovation. https://millionneighborhoods.org/#2/8.84/17.54.

  ↩
- Brelsford, Christa, Taylor Martin, Joe Hand, and Luís M. A. Bettencourt. 2018. “Toward Cities Without Slums: Topology and the Spatial Evolution of Neighborhoods.” *Science Advances* 4 no. 8: 8.

  ↩
- Carneiro, Cláudio, Eugenio Morello, Thomas Voegtle, and François Golay. 2010. “Digital Urban Morphometrics: Automatic Extraction and Assessment of Morphological Properties of Buildings.” *Transactions in GIS* 14 no. 4: 497–531.

  ↩
- Cataldi, Giancarlo, Gian Luigi Maffei, and Paolo Vaccaro. 2002. “Saverio Muratori and the Italian School of Planning Typology.” *Urban Morphology* 6 no. 1: 3–14.

  ↩
- Dibble, Jacob, Alexios Prelorendjos, Ombretta Romice, Mattia Zanella, Emanuele Strano, Mark Pagel, and Sergio Porta. 2016. “Urban Morphometrics: Towards a Science of Urban Evolution.” In *City as Organism. New Visions for Urban Life*, edited by Giuseppe Strappa, Anna Rita Amato, and Antonio Camporeale. Rome, IT: Isufitaly 2015, 22nd ISUF Conference, U+D edition, 14.

  ↩

- Dibble, Jacob, Alexios Prelorendjos, Ombretta Romice, Mattia Zanella, Emanuele Strano, Mark Pagel, and Sergio Porta. 2019. “On the Origin of Spaces: Morphometric Foundations of Urban Form Evolution.” *Environment and Planning B: Urban Analytics and City Science* 46 no. 4: 707–730. https://doi.org/10.1177/2399808317725075.

  ↩
- Fleischmann, Martin, Alessandra Feliciotti, Ombretta Romice, and Sergio Porta. 2020. “Morphological Tessellation as a Way of Partitioning Space: Improving Consistency in Urban Morphology at the Plot Scale.” *Computers, Environment and Urban Systems* 80: 101441. https://doi.org/https://doi.org/10.1016/j.compenvurbsys.2019.101441.

  ↩
- Fleischmann, Martin, Alessandra Feliciotti, Ombretta Romice, and Sergio Porta. 2020. “Morphological Tessellation as a Way of Partitioning Space: Improving Consistency in Urban Morphology at the Plot Scale.” *Computers, Environment and Urban Systems* 80: 101441. https://doi.org/https://doi.org/10.1016/j.compenvurbsys.2019.101441.

  ↩
- Fleischmann, Martin, Ombretta Romice, and Sergio Porta. 2021a. “Measuring Urban Form: Overcoming Terminological Inconsistencies for a Quantitative and Comprehensive Morphologic Analysis of Cities.” *Environment and Planning B: Urban Analytics and City Science* 48 no. 8. https://doi.org/10.1177/2399808320910444.

  ↩
- Fleischmann, Martin, Ombretta Romice, and Sergio Porta. 2021b. "Methodological Foundation of a Numerical Taxonomy of Urban Form." *Environment and Planning B: Urban Analytics and City Science*. https://doi.org/https://doi.org/10.1177/23998083211059835.

  ↩
- Fleischmann, Martin, Ombretta Romice, and Sergio Porta. 2021b. "Methodological Foundation of a Numerical Taxonomy of Urban Form." *Environment and Planning B: Urban Analytics and City Science*. https://doi.org/https://doi.org/10.1177/23998083211059835.

  ↩

- Fleischmann, Martin, Ombretta Romice, and Sergio Porta. 2021b. "Methodological Foundation of a Numerical Taxonomy of Urban Form." *Environment and Planning B: Urban Analytics and City Science*. https://doi.org/https://doi.org/10.1177/23998083211059835.

  ↩
- Fleischmann, Martin, Ombretta Romice, and Sergio Porta. 2021b. "Methodological Foundation of a Numerical Taxonomy of Urban Form." *Environment and Planning B: Urban Analytics and City Science*. https://doi.org/https://doi.org/10.1177/23998083211059835.

  ↩
- Fleischmann, Martin, Ombretta Romice, and Sergio Porta. 2021b. "Methodological Foundation of a Numerical Taxonomy of Urban Form." *Environment and Planning B: Urban Analytics and City Science*. https://doi.org/https://doi.org/10.1177/23998083211059835.

  ↩
- Fleischmann, Martin, Ombretta Romice, and Sergio Porta. 2021b. "Methodological Foundation of a Numerical Taxonomy of Urban Form." *Environment and Planning B: Urban Analytics and City Science*. https://doi.org/https://doi.org/10.1177/23998083211059835.

  ↩
- Fleischmann, Martin. 2019. “Momepy: Urban Morphology Measuring Toolkit.” *The Journal of Open Source Software* 4 no. 43: 4. https://doi.org/10.21105/joss.01807.

  ↩
- Form Based Codes Institute. 2004. “Form-Based Codes Institute at Smart Growth America.” FBCI. https://formbasedcodes.org.

  ↩
- Gatabaki-Kamau, Rose, and Sarah Karirah-Gitau. 2004. “Actors and Interests: The Development of an Informal Settlement in Nairobi, Kenya.” In *Reconsidering Informality: Perspectives from Urban Africa*, edited by M. Vaa and K. Hansen Tranberg, 158–175. Uppsala SE: Nordiska Afrikainstitutet.

  ↩
- Government of Kerala. 2021. “Kerala Municipal Building Rules.” http://lsgkerala.gov.in/htm/kmbr/kmbr_chapter1.html.

↩

- Hakim, Besim S. 2014. *Mediterranean Urbanism: Historic Urban/Building Rules and Processes*. New York, London: Springer.

↩

- He, Kaiming, Xiangyu Zhang, Shaoqing Ren, and Jian Sun. 2016. “Deep Residual Learning for Image Recognition.” 29th IEEE Conference on Computer Vision and Pattern Recognition, Las Vegas, NV, USA, June 27–30.

↩

- Lesiv, Myroslava, Linda See, Juan Carlos Laso Bayas, Tobias Sturn, Dmitry Schepaschenko, Mathias Karner, Inian Moorthy, Ian McCallum, and Steffen Fritz. 2018. “Characterizing the Spatial and Temporal Availability of Very High Resolution Satellite Imagery in Google Earth and Microsoft Bing Maps as a Source of Reference Data.” *Land* 7 no. 4: 118.

↩

- Liu, Penghua, Xiaoping Liu, Mengxi Liu, Qian Shi, Jinxing Yang, Xiaocong Xu, and Yuanying Zhang. 2019. “Building Footprint Extraction from High-Resolution Images via Spatial Residual Inception Convolutional Neural Network.” *Remote Sensing* 11 no. 7: 830.

↩

- Liveable Urbanism. 2021. *Liveable Urbanism Kochi.* Cardiff, UK: Welsh School of Architecture, Cardiff University.

↩

- Maganga, Matthew. 2021. “The Urban Remnants of Colonial Planning in Africa: Dar es Salaam and Nairobi.” *ArchDaily*. Available at: https://www.archdaily.com/968716/the-urban-remnants-of-colonial-planning-in-africa-dar-es-salaam-and-nairobi (accessed 5 May 2022).

↩

- Ministry of Housing, Communities and Local Government. 2021. *National Model Design Code*, edited by MHCLG. London UK: Crown.

↩

- Pan, Zhuokun, Jiashu Xu, Yubin Guo, Yueming Hu, and Guangxing Wang. 2020. “Deep Learning Segmentation and Classification for Urban Village Using a Worldview Satellite Image Based on U-Net.” *Remote Sensing* 12 no. 10: 1574.

↩

- Parolek, Daniel G., Karen Parolek, and Paul C. Crawford. 2008. *Form Based Codes: A Guide for Planners, Urban Designers, Municipalities, and Developers*. Hoboken, NJ: John Wiley & Sons.

↩

- Porta, Sergio, Ombretta Romice, Emanuele Strano, Alessandro Venerandi, Eugenio Morello, Matheus Viana, and Luciano Da Fontoura Costa. 2011. *Plot-Based Urbanism and Urban Morphometrics: Measuring the Evolution of Blocks, Street Fronts and Plots in Cities*. Glasgow UK: Architecture, University of Strathclyde. https://www.researchgate.net/publication/272794921_Plot-based_urbanism_and_urban_morphometrics_measuring_the_evolution_of_blocks_street_fronts_and_plots_in_cities.

↩

- Rokach, Lior, and Oded Maimon. 2005. “Clustering Methods.” In *Data Mining and Knowledge Discovery Handbook*, 321–352. Springer.

↩

- Ronneberger, Olaf, Philipp Fischer, and Thomas Brox. 2015. “U-Net: Convolutional Networks for Biomedical Image Segmentation.” 18th International Conference on Medical Image Computing and Computer-Assisted Intervention, Munich, DE, October 5–9.

↩

- Rousseeuw, Peter J. 1987. “Silhouettes: A Graphical Aid to the Interpretation and Validation of Cluster Analysis.” *Journal of Computational and Applied Mathematics* 20: 53–65.

↩

- Schuegraf, Philipp, and Ksenia Bittner. 2019. “Automatic Building Footprint Extraction from Multi-Resolution Remote Sensing Images Using a Hybrid FCN.” *ISPRS International Journal of Geo-Information* 8 no. 4: 191.

↩

- Sirko, Wojciech, Sergii Kashubin, Marvin Ritter, Abigail Annkah, Yasser Salah Edine Bouchareb, Yann Dauphin, Daniel Keysers, Maxim Neumann, Moustapha Cisse, and John Quinn. 2021. “Continental-Scale Building Detection from High Resolution Satellite Imagery.” *arXiv preprint arXiv:2107.12283*.

↩

- Sirko, Wojciech, Sergii Kashubin, Marvin Ritter, Abigail Annkah, Yasser Salah Edine Bouchareb, Yann Dauphin, Daniel Keysers, Maxim Neumann, Moustapha Cisse, and John Quinn. 2021. "Continental-Scale Building Detection from High Resolution Satellite Imagery." *arXiv preprint arXiv:2107.12283*.

↩

- Venerandi, Alessandro, Ombretta Romice, Olga Chepelianskaia, Kavya Kalyan, Nitin Bhardwaj, Vija Viese, Sebastián Ugás, Shibu Raman, and Sergio Porta. 2021. "Urban Morphometrics and the Intangible Uniqueness of Tangible Heritage. An Evidence-Based Generative Design Experiment in Historical Kochi (IN)." *Heritage* 4: 4399–4420. https://doi.org/https://doi.org/10.3390/heritage4040243.

↩

- Venerandi, Alessandro, Ombretta Romice, Olga Chepelianskaia, Kavya Kalyan, Nitin Bhardwaj, Vija Viese, Sebastián Ugás, Shibu Raman, and Sergio Porta. 2021. "Urban Morphometrics and the Intangible Uniqueness of Tangible Heritage. An Evidence-Based Generative Design Experiment in Historical Kochi (IN)." *Heritage* 4: 4399–4420. https://doi.org/https://doi.org/10.3390/heritage4040243.

↩

- Venerandi, Alessandro, Ombretta Romice, Olga Chepelianskaia, Kavya Kalyan, Nitin Bhardwaj, Vija Viese, Sebastián Ugás, Shibu Raman, and Sergio Porta. 2021. "Urban Morphometrics and the Intangible Uniqueness of Tangible Heritage. An Evidence-Based Generative Design Experiment in Historical Kochi (IN)." *Heritage* 4: 4399–4420. https://doi.org/https://doi.org/10.3390/heritage4040243.

↩

- Wamukoya, M., Kadengye, D. T., Iddi, S., & Chikozho, C. 2020. "The Nairobi Urban Health and Demographic Surveillance of slum dwellers, 2002–2019: Value, processes, and challenges." *Global Epidemiology*, 2, 100024.

↩

- Wang, Jiong, Monika Kuffer, Debraj Roy, and Karin Pfeffer. 2019. "Deprivation Pockets Through the Lens of Convolutional Neural Networks." *Remote Sensing of Environment* 234: 111448.

↩

-

↩

- Xia, Liegang, Xiongbo Zhang, Junxia Zhang, Haiping Yang, and Tingting Chen. 2021. “Building Extraction from Very-High-Resolution Remote Sensing Images Using Semi-Supervised Semantic Edge Detection.” *Remote Sensing* 13 no. 11: 2187.

↩